KU LEUVEN

FACULTEIT WETENSCHAPPEN

Towards the first collection of ^{44}Sc at CERN MEDICIS

Realistic FLUKA simulations of the CERN MEDICIS collection of ^{44}Sc

Bertrand DEWIT

CERN-THESIS-2017-163
30/08/2017

Promotor: Prof. T. E. Cocolios
Instituut voor kern- en stralingsfysica
(KU Leuven)

Begeleider: K. Dockx
Instituut voor kern- en stralingsfysica
(KU Leuven)

Proefschrift ingediend tot het
behalen van de graad van
Master of Science in de Fysica

Academiejaar 2016-2017

Preface

This thesis was written to obtain a Masters degree in Physics at the university of KU Leuven. I was for one year part of the interdisciplinary research group of prof. Thomas Elias Cocolios during which I learned a lot about the ins and outs of a high-level research group.

First and foremost, I would like to thank my supervisor, Kristof Dockx, and promotor, Prof. Thomas Elias Cocolios, for their excellent guidance and support throughout the year. I am also grateful to Simon Stegemann for the advice and help with FLUKA.

I can, of course, not forget my family and friends. They have always been so helpful and supportive during my time studying physics at KU Leuven. In particular, I would like to thank my mother for giving me the opportunity to study and for always standing behind my decisions. My girlfriend, for brightening up my day time after time. Finally, I would like to dedicate this thesis to my father who always supported me in his own peculiar way and was a driving force for me to be able to contribute my small share in medical research.

Scientific summary

CERN MEDICIS (Medical Isotopes Collected form ISOLDE) is a new facility at CERN, with the aim to extract and collect a large range of radioactive isotopes for research and development in medical applications. The ISOLDE (Isotope Separation On-Line Device) facility receives 1.4 GeV protons from the Proton Synchrotron Booster (PSB) where they impinge a target. However, about 85% of them transverse the target without interacting. By placing the MEDICIS target behind the ISOLDE target, a second life is given to these protons. The nuclear interactions inside the target result in a large variety of isotopes. After the irradiation stage, the target is transported to the MEDICIS facility where the off-line extraction is carried out and the radioactive isotope of interest is collected.

The facility includes an experimental hall where employees will be working, even during a batch collection. Since we will be dealing with high activities in the target and the collection point it is of vital importance to evaluate the facility in terms of radiation protection. Exposure to high amounts of radiation can be detrimental for the human body. Therefore, dose limits are set by Swiss legislation and by CERN itself. The facility will need to comply to this limit.

The aim of this thesis is to create realistic simulations of the dose distribution in the experimental hall during the collection of ^{44}Sc. FLUKA, a multi-particle Monte Carlo transport code, is used for this purpose. ^{44}Sc will namely be one of the first isotopes to be collected and was previously determined to be the limiting factor in terms of radiation protection. Doing so, it is possible to determine weak spots in the facility and if any precautions need to be taken. Starting from an initial model of the MEDICIS facility, the model was refined and errors in the geometry were taken out. First, the activated target was included in the geometry. This proved the need of additional shielding in front of a weak spot in the wall separating the target area from the experimental hall. Simulating the expected 1 GBq ^{44}Sc collection showed that the dose rate in the proximity of the collection point exceeds the specified limit. Additional shielding is in this case not a possibility due to limitations in the budget. The proposed solutions are, therefore, demarcation of the area or imposing a limit on the collected ^{44}Sc activity. This limit was determined to be a 0.1 GBq ^{44}Sc collection. Finally it was shown that the accumulation of isotopes on parts of the separator assembly is of no concern, as the resulting contribution to the dose is very low.

Wetenschappelijke samenvatting

CERN MEDICIS (Medical Isotopes Collected from ISOLDE) is een nieuwe faciliteit bij CERN, met als doel het collecteren van radioactieve isotopen voor onderzoek en ontwikkeling van medische toepassingen. ISOLDE ontvangt 1.4 GeV elektronen van de Proton Synchrotron Booster (PSB) waar ze vervolgens op een target terecht komen. 85% van deze protonen gaan echter door het ISOLDE target zonder enige interactie. Door het target van MEDICIS achter dat van ISOLDE te plaatsen wordt er zo nieuw leven gegeven aan deze protonen. De nucleaire interacties die in het target plaatsvinden resulteren in de vorming van een grote verscheidenheid aan isotopen. Na de bestraling wordt het target getransporteerd naar de MEDICIS faciliteit, waarna, door middel van off-line extractie, het gewilde radioactieve isotoop gecollecteerd wordt.

De faciliteit voorziet een experimentele ruimte waarin werknemers aanwezig zullen zijn, zelfs tijdens een collectie. Aangezien we te maken zullen hebben met hoge activiteiten in het target en het collectiepun is het van vitaal belang om de ruimte beoordelen op vlak van stralingsbescherming. Bloodstelling aan hoge mate van radioactiviteit kan namelijk detrimenteel zijn voor het menselijk lichaam. Daarom zijn er dosislimieten opgesteld door zowel de Zwitserse wetgeving als door CERN zelf. De faciliteit zal aan deze limiet moeten voldoen.

Het doel van deze thesis is om realistische simulaties te maken van de dosisdistributie in de experimentele ruimte tijdens de collectie van ^{44}Sc. FLUKA, een multi-deeltjes Monte Carlo transportcode is hiervoor gebruikt. ^{44}Sc zal namelijk één van de eerste isotopen zijn die men zal collecteren en werd eerder bepaald de beperkende factor te zijn in termen van stralingsbescherming. De simulaties maken het mogelijk om zwakke punten in de faciliteit op te sporen en te bepalen of er eventueel maatregelen genomen moeten worden. Beginnend van een initieel model van de MEDICIS faciliteit, werd het model verfijnd en werden fouten in de geometrie weggenomen. Eerst werd het geactiveerde target in het model toegevoegd. Dit toonde aan dat er nood is aan extra afscherming van een zwakke plek in de muur die de target ruimte van de werkruimte afscheidt. Het simuleren van de verwachte 1 GBq ^{44}Sc collectie toonde aan dat de dosistempo in de nabijheid van het collectiepunt de gespecificeerde limiet overschrijdt. Het toevoegen van extra afscherming is in dit geval geen optie door beperkingen in het budget. De voorgestelde oplossingen zijn, daarom, het afbakenen van dat gebied of het invoeren van een limiet op de gecollecteerde ^{44}Sc activiteit. Er werd vastgesteld dat deze limiet een 0.1 GBq ^{44}Sc collectie is. Ten slotte, werd er aangetoond dat de accumulatie van scandium isotopen op delen van de separator geen grote invloed zou hebben, aangezien de resulterende bijdrage aan de dosis zeer laag is.

Vulgariserende samenvatting

De ontdekking van radioactiviteit heeft geleid tot vele nuttige toepassingen. Denk maar aan rookmelders, sterilisatie van voeding en ^{14}C datering. Ook in de medische wereld heeft radioactiviteit zijn weg gevonden, zowel in beeldvorming als in diagnostiek. Zo worden er inwendige of uitwendige bronnen gebruikt om een beeld te vormen van inwendige structuren of om kwaadaardige tumoren te vernietigen. Bij het inwendig toedienen van een radioactieve substantie, wordt een radioactief isotoop gelinkt aan een molecule dat zich op specifieke plaatsen zal ophopen in het lichaam. Op die manier kunnen die delen van het lichaam weergegeven worden of voor therapie bestraald worden. De zoektocht naar nieuwe methodes brengt de vraag naar nieuwe combinaties van molecules en de daaraan gelinkte radioactieve isotopen met zich mee.

CERN MEDICIS is een nieuwe faciliteit in CERN, Genève, met als doel het collecteren van radioactieve isotopen voor onderzoek en ontwikkeling in de medische sector. Het is echter nodig om de verdeling van de radioactiviteit in de werkruimte te beoordelen. Ook al vindt men in radioactiviteit vele positieve toepassingen, kan een te hoge blootstelling eraan, leiden tot negatieve gevolgen. Voorbeelden zijn het rood worden van de huid of verhoogde kans op de vorming van kanker. Daarom zijn er dosislimieten opgesteld voor zulke ruimtes, zodanig dat de negatieve effecten gering blijven.

Deze thesis focust zich voornamelijk op de collectie van het ^{44}Sc isotoop. Aan de hand van simulaties, die de dosisverdeling zo realistisch mogelijk weergeven, wordt er gekeken of er al dan niet behoefte is aan extra afscherming, afbakening van bepaalde zones of het invoeren van een limiet op de collectie.

List of Figures

List of Tables

Contents

Chapter 1

Introduction

1.1 The CERN MEDICIS facility

The ISOLDE (Isotope Separator On-Line Device) radioactive ion beam facility became operational in 1967. Several upgrades took place until it was finally moved to the external beam of the CERN Proton Synchrotron Booster (PSB) in 1991 [1]. The PSB receives protons from a linear accelerator to accelerate them to 1.4 GeV [2]. About 50% of these protons are directed to ISOLDE where they hit a target. The interactions of the protons with the target results in a cocktail of isotopes, both stable and radioactive. They are used to form beams of radioactive nuclei which are subsequently directed to numerous experimental set-ups, e.g. COLLAPS (COLlinear LAser SPectroscopy), CRIS (Collinear Resonance Ionization Spectroscopy) and the IDS (ISOLDE Decay Station) [1, 3, 4, 5]. However, about 85% of the protons pass through the ISOLDE target without interacting and get lost in the beam dump [6]. CERN MEDICIS (MEDical Isotopes Collected from ISOLDE) finds its roots in the idea to give a second life to these protons. Therefore, a second target is placed behind the ISOLDE target. The aim of CERN MEDICIS is to extract a large range of radioactive isotopes and provide them to institutes and hospitals for research in medical applications. Radioactive isotopes are extensively used in both diagnostics and therapy. More specifically, in PET and SPECT imaging for diagnostics as well as α, β and auger therapy. Specific isotopes are often needed in these advanced applications. CERN MEDICIS will be able to offer a wide range of isotopes to cover part of this demand and stimulate further development. The first two columns of table A.1 in appendix A give an overview of the expected isotopes to be collected together with their potential medical application. The estimated in-target and extracted yields are the result of Monte Carlo simulations together with experimental results from ISOLDE [6]. As can be seen, different target materials are used to collect different isotopes, i.e. titanium foils (Ti), yttrium oxide (Y_2O_3), tantalum (Ta) and uranium carbide (UC_x). Following paragraph gives an overview of the operation of CERN MEDICIS.

After irradiating the MEDICIS target in the ISOLDE facility, the isotopes still need to be extracted. The separation and the collection are, however, not carried out in the ISOLDE facility. A new facility, CERN MEDICIS, was built in 2014 for this purpose [6]. A general overview of the area is shown in figure 1.1. The transport of the target to MEDICIS is done with an automatic rail conveyor system, as the target is too radioactive to be handled by a person and takes about 10 minutes. Afterwards, the target is placed

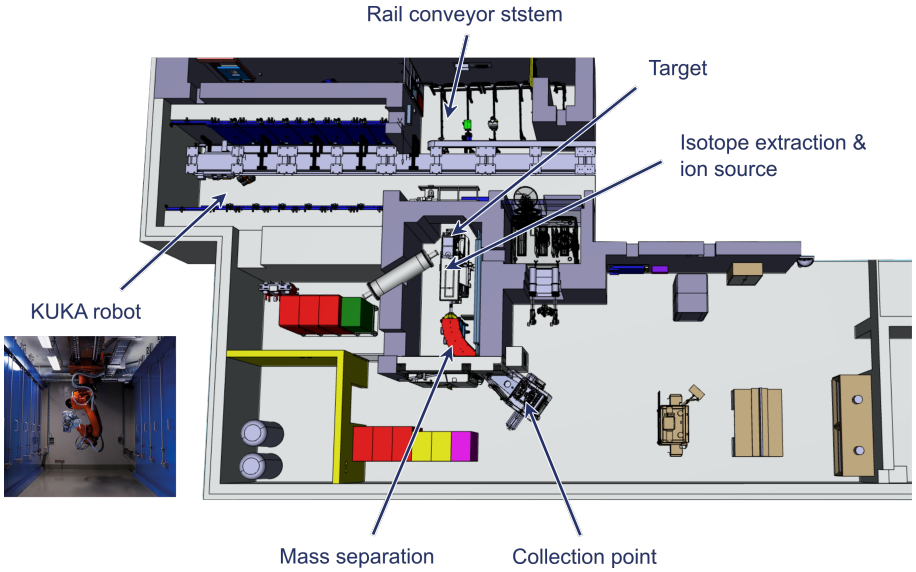

Figure 1.1: *Top view of the CERN MEDICIS facility and its components.*

in a shielded decay and monitoring area by an industrial KUKA robot arm. The storage time depends on the collected isotope (see section 2.1). The robot then places the target into a dedicated hot cell where it is prepared before being connected to the separator.

The isotope extraction can be subdivided in different steps. First of all, the target is heated to high temperatures ($\sim$ 700-2000°C) such that the trapped atoms can diffuse and effuse out of the target into a cavity [1]. Subsequently, the atoms are ionized. This can be done in multiple ways, depending on the element of interest. The simplest set-up is the surface ionization source. Here, the lining material of the cavity has a higher work function than the atom that should be ionized. A surface ionization then occurs when the atom gives off an electron to the walls of the hot cavity. However, if the wanted atom can not be surface-ionized, a plasma ion source is used. Electrons are accelerated into the cavity, which then interact with the atoms and ionize them (see section 2.2). The most element specific ion source is obtained when resonant laser ionization is used to ionize the element of interest. Multiple lasers pass through the cavity. The energies of the lasers are well tuned such that the photon energy coincides with successive electron transitions. As the orbital electron energies are element specific, the energy of the lasers determines which element is ionized, while leaving the others in an electrically neutral state. These ions are then accelerated by means of an electric field, sending them through the mass separator provided by the Centre de Ressources du Cyclotron (CRC) Louvain La Neuve/KU Leuven. Such a mass separator is a dipole magnet whose magnetic field is perpendicular to the path of the ions. The magnetic field bends the particles trajectory into a circular path of which the radius depends on the isotope's mass-to-charge ratio. The heavier the ion, the larger the radius of its path. By introducing slits at the end of the trajectory, a single isotope mass can be selected (see figure 3.8). The isotope is finally collected in the collection chamber where it impinges a material of choice, e.g. a thin metallic foil. Originally, the mass separator from CRC included a switchyard which allows it to collect three isotopes of the same element at once. When the first collections will start, this system will, however, not be operational.

In this way the combination of the resonant laser ionization and mass separation provides a method to collect a single isotope. This should however be nuanced. Nuclei with the same mass, but with a different neutron/proton ratio, can, if they get ionized, reach the collection point. For example, surface ionizations in the hot cavity may also occur during the resonant laser ionization process. This is especially a problem for alkali and alkali earth metals. Due to the low electronegativities of these elements, the high workfunction of the cavity-material can easily extract an electron of the element. After collection further chemical purification can be done, after which the batch is verified and ready to be dispatched. These activities are carried out in the experimental hall, where a dedicated hot cell, glove box and a work bench are available. Figure 1.2 gives a schematic overview of the different steps between target irradiation and transport to a hospital [6].

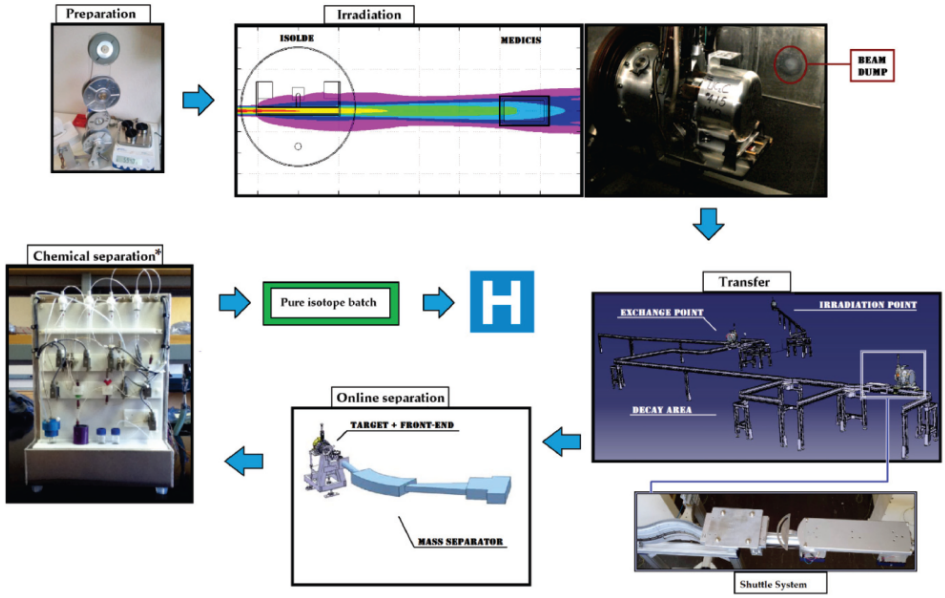

Figure 1.2: *Schematic overview of the different steps in the production of isotopes at CERN MEDICIS. [7].*

1.2 Scope of the dissertation

High levels of radioactivity are involved during the process of collecting isotopes at CERN MEDICIS. As mentioned before, the experimental hall is an area where people will be working. It is thus of great importance to evaluate the radiation dose to these employees. Laws concerning the use of radioactive substances and doses to individuals have been established. These can, for example, imply a limitation on the collected activity to limit the dose to the people. As can be seen on figure 1.1, the collection point is located in the experimental hall itself. This, however, implies the necessity of a hole in the wall, which separates the target area from the experimental hall. Radiation from the target could leak through this opening into the experimental hall. Both the collection point and the target can thus be important contributors to the radiation dose.

This dissertation mainly focuses on the collection of ^{44}Sc. A first reason for this choice is that during the initial stage of collection at CERN MEDICIS, only low Z target materials will be used, i.e. Ti and Y_2O_3. ^{44}Sc will, therefore, be one of the first isotopes to be collected (table A.1 [6]). ^{44}Sc has also previously been identified as the limiting case in terms of radiotoxicity and is therefore the ideal case to evaluate the dose distribution in the experimental hall [8]. The aim is to create realistic simulations of the dose distribution in MEDICIS's experimental hall during a ^{44}Sc collection. Both the target and the collection point need to be taken into account and will determine the necessity of extra shielding. Besides ^{44}Sc, the other scandium isotopes which impinge the slits after mass separation need to be considered as these slits do no not get replaced after every batch collection. Hence, a build-up of activity could lead to high dose levels after long term use.

Chapter 2

Theoretical background

2.1 Radioactive isotope production and decay

2.1.1 High energy nuclear reactions

The production of radioactive isotopes at CERN MEDICIS is governed by the bombardment of a target with high energy protons (1.4 GeV). At these energies the main interactions will be spallation, fragmentation and even fission in heavier targets like uranium carbide. The result of these reactions is the creation of a large variety of nuclei covering a large range in proton/neutron ratio [9].

Spallation is generally described by a sequence of three stages: the intra-nuclear cascade, followed by a pre-equilibrium stage and finally de-excitation. For high energy protons (>100 MeV), the de Broglie wavelength becomes smaller than the average distance between nucleons in the target nuclei ($\sim$1 fm). It is, therefore, assumed that the incoming proton directly interacts with the nucleons through a series of two body interactions, as is illustrated in figure 2.1 [10]. This is the "intra-nuclear cascade" and takes place within a time scale of $\sim 10^{-22}$ s. The initial proton interacts with one of the nucleons, a proton or a neutron, through elastic collisions, which on their part can interact with the other nucleons. If the energy exceeds several hundred MeV, pion production becomes possible. At even higher energies (several GeV) heavier hadrons can be produced [11]. These particles can also participate to the interactions within the nucleus, creating a cascade of interactions. Particles that gained enough energy to escape the nucleus are subsequently emitted, while the remaining nucleus is left in a highly excited state. The particles are not ejected isotropically, but mainly focussed in the direction of the incoming proton.

Before the de-excitation of the remaining nucleus, a pre-equilibrium stage is defined [10]. Although the particles are still interacting within the nucleus, the energy of the particles have reached a lower limit (tens of MeV). The nucleus is however still not in thermal equilibrium. More high energy fragments, e.g. protons and neutrons, may be emitted from the core while reaching equilibrium. During the subsequent de-excitation stage, the nucleus is able to dissipate its energy in several ways, i.e. nuclear evaporation, fission and gamma emission, depending on the remaining energy and mass of the nucleus. During evaporation, light fragments (e.g. ^{2}H,^{3}H,^{4}He) and neutrons with an energy of several MeV are emitted from the excited nucleus. In this stage the emission is isotropic, in contrast

to the intra-nuclear cascade. In case of heavy targets ($Z \gtrsim 65$), fission is able to compete with evaporation during the nuclear de-excitation. The nucleus splits into two fragments, accompanied by the release of neutrons. If the excitation energy of the nucleus is too low to initiate either of previous methods (<8 MeV $\sim$ neutron binding energy), the nucleus will de-excite by γ-emission [11]. Figure 2.2 gives a schematic overview of a spallation reaction.

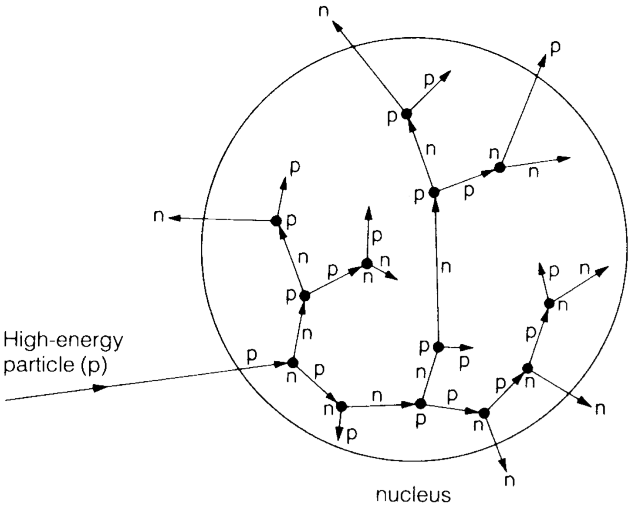

Figure 2.1: *Illustration of the intra-nuclear cascade as a first stage in a spallation reaction [12].*

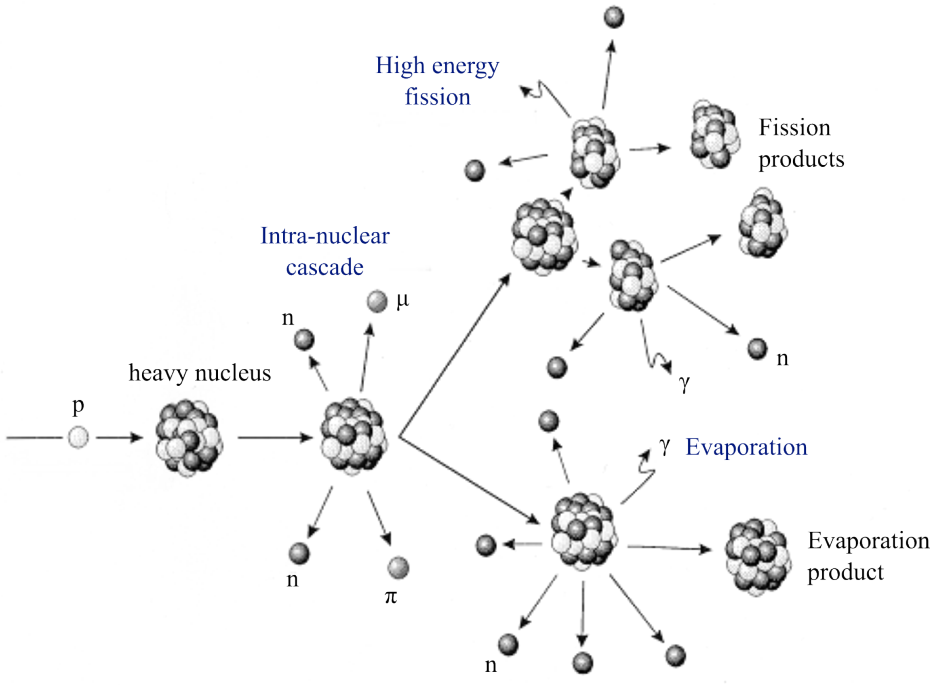

Figure 2.2: *Schematic overview of a spallation reaction [13].*

A fragmentation reaction can be described as the break-up of an excited nucleus, taking place before the energy equilibration in the nucleus [14]. The reaction is often explained by the "abrasion-ablation" model. In this simple model it is assumed that the incoming high energy particle shears off part of the target nucleus during a peripheral interaction. The result is the formation of two highly excited fragments, a large one and a small one, with a proton/neutron ratio similar to the parent nucleus. Subsequently, the excited fragments are able to de-excite by particle evaporation. As the fragments are thus neutron rich, the evaporation mostly consists of neutron emission [12].

Reaction products

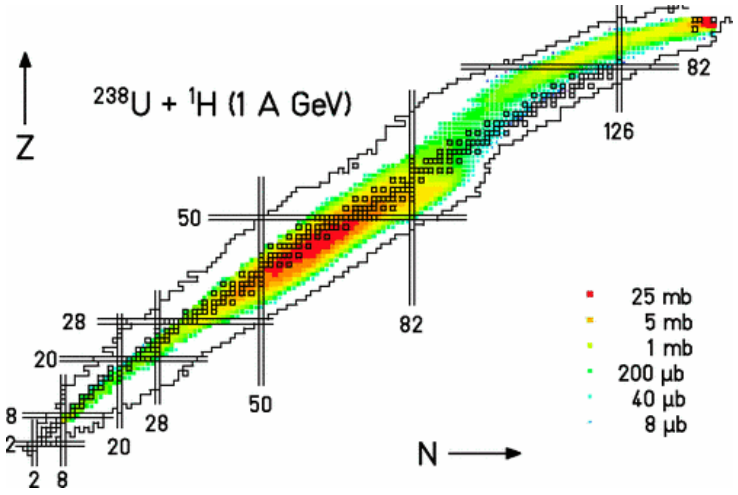

Figure 2.3: *Residual nuclei produced by the interaction of 1GeV protons with a 238U target and a cross section larger than 8 mb. The stable isotopes and the neutron and proton drip line are respectively indicated with empty squares and the surrounding border. The double horizontal and vertical lines indicate the magic numbers [15].*

Figure 2.3 illustrates the range of isotopes produced after the irradiation of a ^{238}U target with 1 GeV protons on the nuclear chart. The colors denote the probability that the isotope is created and is thus proportional to the in-target yield. This probability corresponds to the cross section, σ, with "barn" ($=10^{-28}$ m^2) as its unit. Similar results are expected for the uranium carbide target at MEDICIS, as the irradiation conditions are comparable. Three groups can be distinguished [9]. In the high mass region, a group of isotopes is located to the left of the line of stability, indicating neutron deficiency. These isotopes are the remnants of spallation-evaporation reactions, and is sometimes called the "evaporation corridor". The neutron deficiency is due to the coulomb barrier being only felt by protons. During the evaporation process, neutrons are thus more likely to be expelled from the nucleus, leading to a higher proton/neutron ratio. In the central mass region, a group of isotopes with high cross sections is observed on the right of the line of stability. These are the result of fission during the spallation process. The neutron excess of these isotopes is the consequence of the low proton/neutron ratio of stable heavy elements (e.g. p/n(^{238}U)=0.63) compared to medium and low mass isotopes (e.g.

p/n(^{103}Rh)=0.78) [16]. The proton/neutron ratio of the parent nucleus remains virtually preserved during the fission proces, thereby producing neutron rich isotopes. The excess neutrons can, however, be ejected in more energetic fission processes. In such a case, pre- and post-fission neutron evaporation reduces the number of neutrons and broadens the range of isotopes. The third group is observed as a tail of lighter nuclei behind the fission residues. The production cross section for these isotopes increases for increasing mass and are produced by fragmentation [9].

For the titanium target, used for the production of ^{44}Sc, the situation is slightly different. First of all, titanium (Z=22) is much lighter than uranium (Z=92). Therefore, the whole range of isotopes in the high and intermediate mass regions as described before will not be produced during the irradiation. Uranium is, on the other hand, also fissionable, which is not the case for titanium. This means that, for the titanium target, the isotopes are a result of spallation and fragmentation. In the end, the wider range of isotopes produced in the heavy uranium target, implies an increased radiotoxicity.

2.1.2 Radioactive decay

As discussed in the previous section, many of the produced isotopes are not necessarily stable. The unstable nuclei lose excess energy by emitting radiation under various forms, e.g. α-particles, electrons, positrons, etc. [17]. Radioactive decay is a stochastic process characterised by an isotope specific decay constant λ [s^{-1}]. The rate of decay is given by

$$\frac{dN}{dt} = -\lambda N = A. \tag{2.1}$$

Here, N denotes the number of radioactive nuclei and A the activity [Bq]. The decay rate leads to a property of a radioactive isotope, known as the "half-life", $\tau_{1/2}$ [s]. It is defined as the time it takes for half of the initial amount of isotopes to decay and is related to the decay constant by $\tau_{1/2} = \ln(2)/\lambda$. Table A.1 gives the half-life of each isotope expected to be collected at CERN MEDICIS.

Isotopes with a neutron or proton excess are prone to β^- and β^+ decay, respectively. During β^- decay one of the neutrons (n) is converted into a proton (p) together with the creation of an electron (e^-) and an electron-antineutrino ($\bar{\nu}_e$):

$$n \rightarrow p + e^- + \bar{\nu}_e. \tag{2.2}$$

As this is a three-body process, the electron's energy is not a fixed value, but a continuous function with an endpoint energy equal to the total decay energy. A representative energy spectrum is shown in figure 2.4. A wide range of half-lives are observed for β^- decaying isotopes. The most unstable nuclei, close to the drip line, have half-lives in the order of nanoseconds, while other isotopes can have half-lives in the order of thousands of years. β^+ decay is similar to β^- decay, with the main difference being the conversion of a proton compared to a neutron. The proton is converted into a neutron accompanied with a positron (e^+) and an electro-neutrino (ν_e):

$$p \rightarrow n + e^+ + \nu_e. \tag{2.3}$$

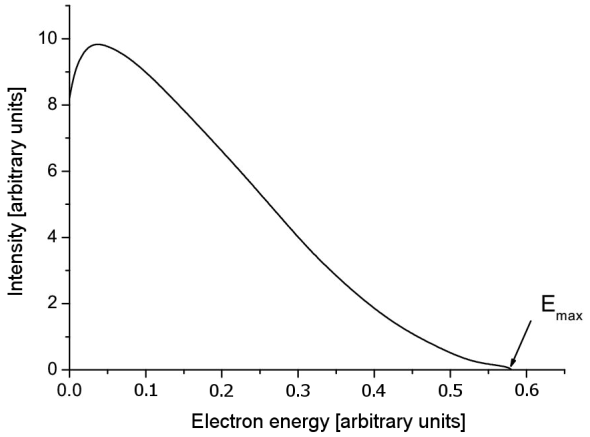

Figure 2.4: *Representation of a β^- decay electron energy spectrum.*

After β decay, the nucleus is often left in an excited state. Subsequent de-excitation by emission of γ-rays is, therefore, often observed for β decaying isotopes. A competing process to γ decay is internal conversion. The excess energy is then transferred to one of the orbital electrons, most often a K- or L-shell electron. The energy of the electron is equal to the difference between the excitation energy and the binding energy of the electron. A proton can, alternatively to β^+ decay, in some isotopes be converted into a neutron, by capturing an orbital electron. This process is, therefore, appropriately named "electron capture" (EC). The inner orbital electrons (e.g. K- or L-shell electrons) have a non-zero probability of being in the nucleus. The interaction of the electron with the proton can then lead to following process:

$$p + e^- \rightarrow n + \nu_e. \tag{2.4}$$

The capture of the orbital electron results, however, in a vacant space in one of the orbitals. Electrons from higher energy orbitals cascade down to fill in the vacant place, thereby emitting characteristic x-rays.

α decay occurs in heavy isotopes which are unstable against the emission of a ^{4}He-nucleus (α-particle). The energy of the α-particle is mono-energetic, in contrast to the electron's energy spectrum from β decay, and ranges generally between about 4 to 6 MeV. Concerning the half-life, a correlation is observed with the energy of the α-particle. In general, the higher the energy, the shorter the half-life. They range from milliseconds (10^{-3} s) to 10^{10} years. Figure 2.5 shows how an isotope evolves on the nuclear chart for the different types of decay.

As a consequence of this radioactive decay, the isotope composition in the target is a function of time. For the collection of some isotopes it may therefore be beneficial to store the target for a certain amount of time. If the wanted isotope is the daughter product of a well produced shorter lived nucleus, the specific activity of that isotope will rise. In some cases, the beam that reaches the collection chamber does not contain the isotope that will eventually be used in the medical application. Instead a mother isotope

is collected. The following decay chain is an example of the production of ^{152}Tb. ^{152}Er is collected, which ends up as ^{152}Tb through a series of β^- decays.

$$^{152}Er \xrightarrow[10.3\text{ s}]{\beta^-} {}^{152}Ho \xrightarrow[161.8s]{\beta^-} {}^{152}Dy \xrightarrow[2.38h]{\beta^-} {}^{152}Tb \tag{2.5}$$

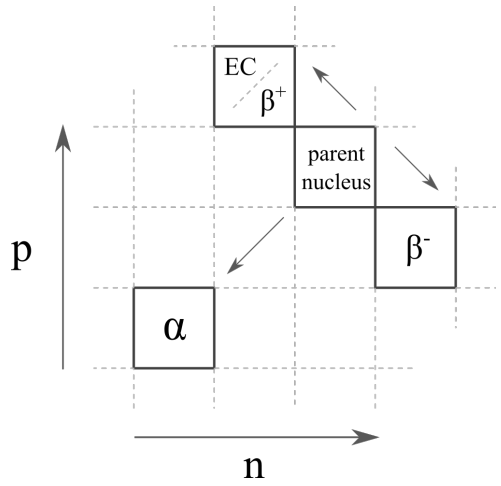

Figure 2.5: *A schematic overview of the different types of decay on the nuclear chart.*

2.2 Interactions of radiation with matter

Insight in the theoretical and practical side of radiation protection can only be achieved by obtaining a profound understanding of the interaction of radiation with matter. It are these interactions that form the basis of shielding, quantitative and qualitative measurements of radiation and the evaluation of biological consequences of exposure to radiation. In most cases they go along with a transfer of energy to the medium it impinges. The interaction probability and amount of energy transferred depends on multiple factors, e.g. the type and energy of the incoming radiation and the type of interacting particle, i.e. nucleus or electron. A more detailed description of the different interactions will be discussed in following paragraphs in which a first distinction is made between charged and uncharged particles.

2.2.1 Charged particles

Electrons, α-particles, protons and heavy ions all fall in the category of charged radiation. Due to the charged nature of these particles, the coulomb interaction plays an important role in the way they interact within the medium. The moving particle continuously interacts with the negatively charged orbital electrons, effectively transferring part of its energy during each interaction. Although interactions with the atomic nuclei are also possible, they are far less likely to occur. Therefore, these type of interactions will not play a significant role in most practical applications [17]. As an orbital electron gains energy via the Coulomb interaction when a charged particle passes by, two possible outcomes present themselves. The first option is that the transferred energy is not large enough to excite the electron to the continuum and the atom is left in an excited state. If, on the other hand, the energy is large enough, the electron is stripped from the atom and is ionized. In this way the charged particle leaves a path of positive ions and electrons behind. In some instances the energy transferred to the electron is sufficient for it to further ionize atoms along its path. Such an occurrence is called a δ-ray [18]. Another way for particles to lose energy is by radiative processes. This is however only an important factor for electrons. The overall effect of many transfers of small amounts of energy is that the charged particle slows down and eventually comes to a stop. This deceleration is described by the stopping power, S, denoting the rate of energy loss per unit of distance [17]. Different descriptions are needed for electrons and heavy charged particles, i.e. α-particles, protons and heavy ions. This discrepancy originates from radiative energy losses coming into play for electrons. One also needs to take into account the indistinguishability of the fast electron and the atomic electron. In what follows, heavy charged particles and electrons are discussed separately.

2.2.1.1 Heavy charged particles

For heavy charged particles the stopping power is defined as

$$S = -\frac{dE}{dx} = \frac{4\pi e^4 z^2}{m_0 v^2} NZ \cdot \left[\ln\left(\frac{2m_0 v^2}{I}\right) - \ln\left(1 - \frac{v^2}{c^2}\right) - \frac{v^2}{c^2} \right]. \tag{2.6}$$

In the right expression z and v denote the atomic number and velocity [c] of the charged radiation, e and m_0 the charge [e] and rest mass [eV/c^2] of an electron, N and Z the

atomic density [m^{-3}] and atomic number of the medium and, finally, I is the average energy necessary to ionize or excite an atom in the medium [eV]. This formula is known as the Bethe formula [17]. In non-relativistic situations ($v/c \ll 1$) only the first term in the brackets is of significance. For heavy charged particles originating from decay such a non-relativistic situation can be assumed [19]. With accelerators, however, relativistic velocities can be achieved. Equation 2.6 shows an inverse proportionality with v^2. The deceleration, therefore, increases as the particle slows down, releasing most of its energy at the end of its path. A quadratic relation is observed between the stopping power and the charge of the particle. A higher charge leads to a stronger Coulomb interaction, resulting in a larger stopping power. The properties of the medium are incorporated in the atomic density, N, and the atomic number of the medium, Z. This boils down to the electron density in the medium. Furthermore, another property of the medium, the ionization potential of the medium, I, is incorporated in the logarithmic term. An increased electron density means that more interactions can take place, resulting in a higher stopping power. One should however be aware that the Bethe formula assumes that the particles move fast enough such that they are stripped from their atomic electrons. This assumption does not hold throughout the whole trajectory of the particle, more precisely at the end of the path where they have lost most of their energy. At these lower energies the particles will bind electrons, effectively reducing the charge and thereby also the stopping power. This gradual rise followed by the sudden drop in stopping power forms a peak at the end of the particle's track. This feature is called a Bragg peak. Figure 2.6 shows this overall trend of the stopping power for both one single α-particle and a parallel mono-energetic beam of α-particles. The broadening of the peak in the case of a parallel beam is caused by energy straggling. Even though the particles in the beam have the same initial conditions, the details of the interactions will very slightly for each particle. As a result, there is also a slight variation in the path lengths, giving rise to the spread in the peak.

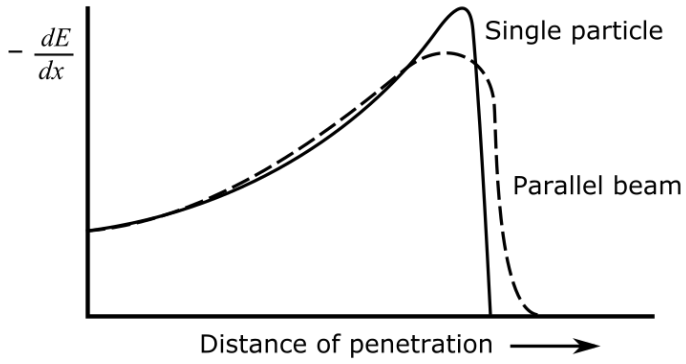

Figure 2.6: *The general shape of the stopping power as a function of penetration distance, shown both for a single α-particle (solid line) and a parallel beam of α-particles (dashed line). A peak is observed at the end of the track, the Bragg peak. The spreading in the bragg peak for a parallel beam is due to energy straggling [17].*

The stopping power leads to another important quantity, namely the range of the incident radiation in a medium. The range is the depth at which the particle comes to rest in a medium. If the initial energy and characteristics of the particle are known such that

the stopping power can be calculated along its path, a crude approximation of the range can be made. This is done in the continuous-slowing-down approximation (CSDA) [20], calculated as

$$d_{CSDA} = \int_0^{E_0} \frac{1}{S(E)} \mathrm{d}E. \tag{2.7}$$

With E_0 being the initial energy of the incoming particle and $S(E)$ the energy dependend stopping power. This approximation assumes that the particles travel in a straight line. In this way, the range coincides with the path length. The large mass of a heavy charged particle compared to the atomic electrons with whom they interact (a proton is approximately 1836 times heavier than an electron [21]), results in only very small deviations from their initial path after an interaction. The maximal elastic scattering angle is namely equal to $arcsin(m_e/M)$, with M being the mass of the incomming particle and m_e the atomic electron's mass. For high M, the angle becomes smaller. Therefore, the assumption of a straight track is in this case valid. As an example, an α-particle with an energy of 10 MeV has a range of approximatly 10 cm in air, but only 0.1 mm in human tissue [20, 22]. For protons these values are 120 cm and 1 mm respectively. This shorter range in tissue for α-particles can be explained by looking at the Bethe formula. An α-particle is essentially an helium nucleus, consisting of two protons and two neutrons, possessing a charge of 2 e. This twofold charge increases the stopping power with a factor of four compared to a proton (1 e), when implemented in equation 2.6. For a given energy, the α-particle's velocity is slower than a proton's due to the larger mass, again resulting in a larger stopping power.

2.2.1.2 β-particles

A β-particle can both refer to an electron or a positron. The later, positrons, annihilate at the encounter of an atomic electron, producing two back-to-back photons with an energy of 511 keV. This conversion to uncharged radiation happens almost instantly, therefore we will now only focus on electrons.

For electrons two ways of energy loss present themselves, by collisions and by the emission of electromagnetic radiation. Consequently, the stopping power is divided in two terms. The first term, the collisional energy loss, is equivalent to the energy loss as seen for heavy charged particles. However, equation 2.6 requires a modification to accommodate the indistinquishability of the fast electron and the atomic electron during an interaction. The modified equation, the collisional specific energy loss for electrons, becomes

$$\begin{aligned} -\left(\frac{dE}{dx}\right)_c = \frac{2\pi e^4 NZ}{m_0 v^2} \Bigg[\ln \frac{m_0 v^2 E}{2I^2(1-\beta^2)} - (\ln 2)\left(2\sqrt{1-\beta^2} - 1 + \beta^2\right) \\ +(1-\beta^2) + \frac{1}{8}\left(1-\sqrt{1-\beta^2}\right)^2 \Bigg]. \end{aligned} \tag{2.8}$$

With $\beta = v/c$ and all other variables equal to those in equation 2.6. The second term in the stopping power includes the radiative energy loss. Electromagnetic radiation is emitted when a charged particle is accelerated. In our case this acceleration corresponds to the

deflection of the incoming electron during an interaction. Such electromagnetic radiation is named Bremsstrahlung. The production of Bremsstrahlung is inversely proportional to the square of the mass of the incoming charged particle. This is also the reason why this radiational energy loss term is not included for heavy charged particles ($m_p \gg m_e$). The stopping power is also proportional to the energy E of the incoming particle and the atomic number Z of the medium. The radiative energy loss is given by

$$-\left(\frac{dE}{dx}\right)_r = \frac{NEZ(Z+1)e^4}{137m_0^2c^4}\left(4\ln\frac{2E}{m_0c^2} - \frac{4}{3}\right). \tag{2.9}$$

In contrast to the heavy charged particles, the path of electrons is not straight. For two identical particles the maximal scattering angle as defined in the section for heavy particles becomes equal to 90°. Interactions between the fast electron and the atomic electrons thus results in a scattered path. The CSDA range is in this case an overestimation, as the requirement of a straight path is not fulfilled. It is however a good approximation of the total path length of the electron. The penetration depth of a 10 MeV electron in air is approximately 10 m and in human tissue approximately 1 cm [20].

2.2.2 Uncharged Particles

In bright contrast to the charged radiation, uncharged particles like photons and neutrons will not continuously interact with the surrounding medium, as is the case for charged particles. Instead, a few distinct interactions take place in which all or a part of the energy is transferred. It is thus a stochastic process in which each interaction has a certain probability to take place. This means that there is always a non-zero probability that a photon passes a substance without any interaction at all, an important consideration for protective purposes. An interaction can result in the production of charged particles which on their turn then cause excitations and ionizations as discussed in the previous section. Therefore uncharged radiation is sometimes called "indirect ionizing radiation". Examples of this uncharged radiation are photons and neutrons, they will be separately discussed in further detail.

2.2.2.1 Photons

A photon can interact with its surrounding in different ways, i.e. the photo-electric effect, Compton scattering, pair production and Rayleigh scattering [17]. The three first interactions lead to the creation of secondary electrons which in their turn can deposit energy in the medium. Rayleigh scattering, however, does not directly generate secondary electrons. In what follows, a short description of each type of interaction is given.

In case of the photo-electric effect, the photon completely disappears during the interaction. All of the energy of the photon (hv) is transferred to an orbital electron, effectively ejecting it from the atom. Some energy is needed to overcome the initial binding energy of the electron. The electron energy, E_{e^-}, is thus equal to $E_{e^-} = hv - E_b$, with E_b the binding energy. This binding energy varies for different electron shells, e.g. K-shell, L-shell, ..., with the K-shell having the highest binding energy. For K-shell electrons, which have the highest photo-electric cross section, the binding energy ranges from a few eV (e.g. 13.6 for hydrogen) to a few hundred keV for heavier elements (e.g. 115 keV for uranium) [23].

In addition to the electron, an ion with a vacancy in one of its orbitals is left behind. The vacancy in an inner shell e.g. the K-shell, is then filled by an higher energy electron from another shell e.g. the L-shell. This creates a cascade of electrons falling down to lower energy states. During that process, the energy can be released in two competitive ways. Firstly by the emission of characteristic x-rays. These are often absorbed close to their place of origin, but there is again the possibility that they escape from the material. The second competing process is the ejection of an Auger electron. The released energy is in that case transferred to one of the other orbital electrons. After the rearrangement of the orbital electrons, the ion is able to quickly take up a free electron. Figure 2.7 shows the cross section for the photo-electric effect in tungsten, along with the other interactions, as a function of the photon's energy. An inversely proportional relation regarding the energy can be seen, along with a predominance at relatively low energies. The sudden discontinuity in the curve is caused by the discrete binding energies of the different electron shells. Once the energy of the photon is high enough to overcome the binding energy of a new shell, e.g. a K-shell electron, the cross section suddenly rises as an extra electron can participate in the interaction. Figure 2.8 pours the dependency of the three main interactions on the energy, hv, and the atomic number, Z, of the absorbed material into one graph. Each line indicates the conditions at which interactions are equally probable. The photo-electric effect is situated at the left side of the first line, indicating its importance at lower energies. For increasing Z, figure 2.8 also shows a gain in dominance over the Compton effect. The photo-electric probability, τ, reflects these dependencies as follows:

$$\tau \cong constant \times \frac{Z^n}{E_\gamma^{3.5}}. \tag{2.10}$$

The exponent n varies between 4 and 5 over the energy range of interest.

A photon undergoing Compton scattering will only transfer part of its energy to an orbital electron of the absorber material. The end result is a free electron, the "recoil electron", and a photon with a lower energy. Both the electron and the photon are emitted at a specific angle with respect to the original photon, depending on the amount of energy transferred during the interaction. The angle between the direction of the initial photon with an energy hv and the scattered photon with energy hv' is called the "scattering angle", θ. By using the laws of conservation of momentum and energy, an expression relating the energy transfer and the scattering angle can be found. This relation is given by:

$$hv' = \frac{hv}{1 + \frac{hv}{m_0c^2}(1 - cos\theta)}. \tag{2.11}$$

Where m_0 is the rest mass of an electron. For large θ, a large portion of the energy is transferred to the recoil electron. However, even if $\theta = 180°$, hv' is not equal to zero and some energy is left in the scattered photon. Figure 2.7 together with figure 2.8 show that Compton scattering is only important in the intermediate energy range for high Z materials and wider range for low Z materials. The Compton scattering probability is denoted by σ and is independent on the atomic number Z. Compton scatter is the predominant interaction for most γ-ray's emitted by radioactive isotopes.

At energies above 1022 keV, equal to the sum of the rest masses of a positron and an electron, pair production becomes possible. Near an atomic nucleus, the energy of such a photon can be converted into an electron-positron pair. Even if the energy of the photon exceeds 1022 keV, all the energy is transferred. The excess ends up as kinetic energy shared by the electron and the positron. The pair production probability is denoted by κ. As shown in figure 2.7, the pair production probability, κ, increases rapidly with increasing photon energy. κ is also approximately proportional to the square of the atomic number of the absorber material. Figure 2.8 indeed shows an increasing importance of pair production at higher energies and higher atomic number.

Finally, Rayleigh scattering, also called "coherent scattering", is a possible interaction for a photon in an absorber material. Contrary to previous interactions, Rayleigh scattering does not create free electrons. The atom with whom the photon interacts does not get excited nor ionized. The energy of the photon remains the same, but its direction changes. Although this type of interaction is not important regarding energy deposition in soft tissue and its biological implications, it is important to incorporate the possibility of a change in direction when it encounters a material, e.g. shielding. In this way it may contribute to the creation of hotspots in certain places. The Rayleigh scattering probability becomes more prominent at relatively low energies, as shown in figure 2.7.

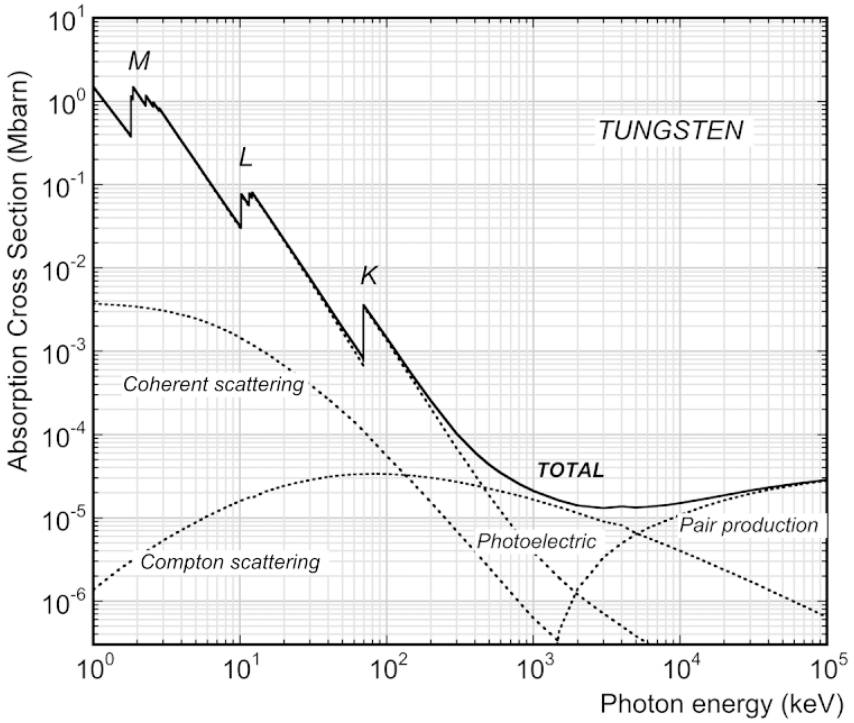

Figure 2.7: *Energy dependence of the different photon interactions in tungsten [24].*

Contrary to the charged radiation, the definition of the range of a photon in a medium is undefinable. Some photons will not even interact with the medium due to the stochastic nature of the interactions. Photon radiation is therefore highly penetrating. To characterize the penetrability, the quantity Half Value Layer (HVL) is used instead of the

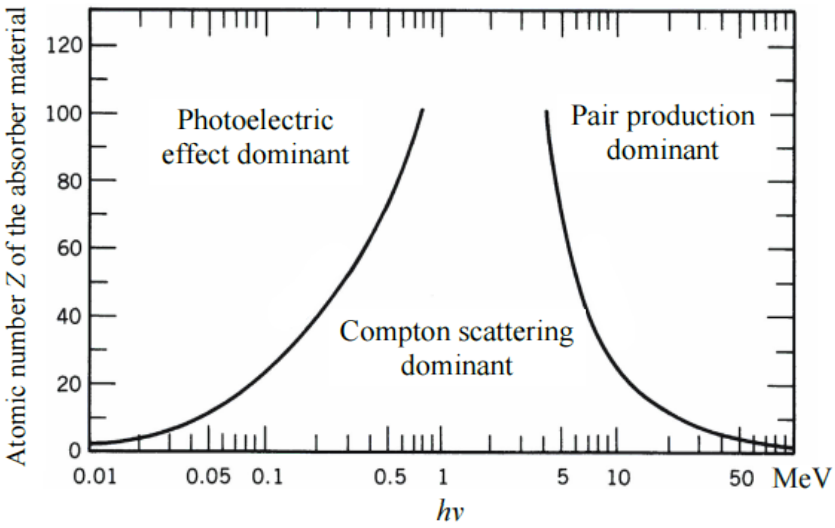

Figure 2.8: *Dominant photon interactions as a function of photon energy (hv) and atomic number of the medium (Z) [17].*

range for charged particles. The HVL is defined as the thickness of the material needed to reduce the initial intensity by a factor two. Previous paragraphs explained the ways in which a photon can be taken out of a beam when penetrating a material. By adding up the probability of each interaction, we find the probability per unit of path length that the photon is removed. This quantity is also called the "linear attenuation coefficient", denoted with μ [m^{-1}]. In other words,

$$\tau + \sigma + \kappa = \mu. \tag{2.12}$$

The linear attenuation coefficient is thus a material (Z) and energy (hv) dependent quantity. The relation between the linear attenuation coefficient and the HVL is given by:

$$\frac{N_{\gamma_0}}{2} = N_{\gamma_0} e^{-\mu \cdot HVL}. \tag{2.13}$$

Or, after some rearrangement:

$$HVL = \frac{\ln(2)}{\mu}. \tag{2.14}$$

Here N_{γ_0} is the number of initial photons in the beam. The exponential decrease in the number of photons finds its root in the stochastic nature of the interactions. The HVL is an important factor in the design of shielding. In case of a large HVL, or equivalently a small linear attenuation coefficient, the thickness of the shielding would become impractically thick.

2.2.2.2 Neutrons

Hitherto almost all interactions of the impinging radiation involved orbital electrons. Neutrons on the other hand, interact with the atomic nuclei of the medium. Typically a distinction is made between fast and slow neutrons as the interaction probability of the types of interactions vary dramatically with neutron energy [17, 25]. At around 0.5 eV a sudden drop in the neutron absorption cross section of cadmium is observed. This energy

is used to define the distinction between fast and slow neutrons. Figure 2.9 shows the ^{113}Cd neutron absorption cross section as a function of the neutron energy. The dashed line indicates the separation between the two regimes. Multiple successive peaks can be seen in the fast regime. These coincide with resonance states of the nucleus. In such a case, the transferred energy coincides perfectly with the discrete energy states of the nucleus [26].

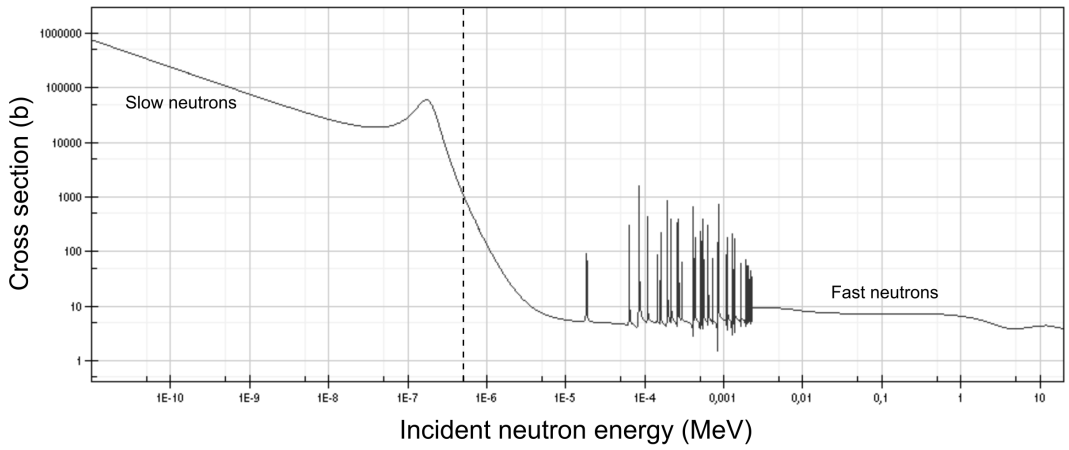

Figure 2.9: *The neutron absorption cross section for ^{113}Cd as a function of the incident neutron energy. The dashed line indicates the region where the cross section suddenly drops, separating the slow and fast neutron cross section regime [27].*

For slow neutrons, the two main interactions are inelastic scattering and neutron induced nuclear reactions. As these neutrons do not possess a lot of energy to begin with, each inelastic interaction will consist of only a very small transfer of energy. However, these interactions are likely to happen and lower the energy even more. Eventually the neutron will reach thermal equilibrium (e.g. $\pm 0.025\ eV$ at room temperature). These thermal neutrons can get captured by a nucleus, inducing a nuclear reaction. These reactions often result in the emission of a photon. Other possible reactions result in the emission of an α-particle, proton or fission fragments. In terms of radiation protection, the reaction accompanied with the emission of a photon is important as it is often the most probable one. Furthermore, the produced photons are harder to attenuate compared to the heavy particles resulting from the other reactions.

Neutron induced nuclear reactions do not play a significant role at higher neutron energies. However, fast neutrons do possess enough energy to transfer a substantial amount of energy to a nucleus during elastic scattering. The nucleus will recoil and is able to ionize atoms along its path, effectively becoming the secondary radiation particles of the fast neutrons. During each interaction the neutron loses some of it interaction and slows down. The maximal energy transfer depends on the mass of the nucleus and the energy of the neutron. For non-relativistic neutrons ($E \ll 939\ MeV$), the maximum fractional energy transfer for neutron elastic scattering is given by [17]

$$\left.\frac{E_R}{E_n}\right|_{max} = \frac{4A}{(1+A)^2}. \tag{2.15}$$

Here, E_R denotes the recoil energy of the nucleus, E_n the neutron energy, and A the number of nucleons. For a hydrogen nucleus, with $A = 1$, equation 2.15 shows that all the neutron energy can be transferred in one interaction. For increasing A, the maximal possible energy transfer gets smaller. Light nuclei are therefore most effective at slowing down fast neutrons. In some neutron interactions, the recoiled nucleus may be left in an excited state after which it will decay by emitting a photon. This is important to take into consideration for radiation protection purposes.

2.3 Biological effects

To acquire insight on the damaging effects of ionizing radiation on a living organism, one has to assess the damage on three different levels. The eventual damage to tissue and organs is in the end the result of damage to the cells out of which they consist. This cell damage is in its turn the outcome of damage to the constituents of the cell caused by ionizing radiation. Damage on the sub-cellular level will thus potentially lead to damage on the cellular level, possibly resulting in tissue damage or genetic defects. Just as in a normal material, ionizing radiation causes excitations and ionizations along its path. These transfers of energy can break intramolecular bonds. In this way, the functionality of the molecule can alter or disappear completely. In a cell, a distinction can be made between two groups of constituents with which the radiation may interact. On the one hand DNA (Deoxyribonucleic acid), and on the other hand all the other constituents, e.g. cell organelles, proteins, enzymes, etc. These cell organelles, proteins and so on, are generally very efficiently replaced by the cell in case of damage. Therefore these interactions do not really affect the survival chances of a cell. DNA-damage, however, can have drastic consequences. DNA is a macromolecule located in the nucleus of eukaryote cells (as is the case for humans), and contains the genetic code determining the characteristics of an organism. The structure of DNA resembles a double helix, made up of so called "nucleotides". Each nucleotide consists of a sugar called "deoxyribose", a phosphate group and one of four nucleobases, being adenine, cytosine, guanine or thymine. These nucleobases form adenine-thymine and cytosine-guanine pairs by forming hydrogen bonds [28]. More specifically, three hydrogen bonds between cytosine and guanine, and two bonds between adenine and thymine. It is the sequence of these base pairs that forms the genetic code. Figure 2.10 illustrates this structure. In this way DNA contains the instructions to make molecules, i.e. proteins, necessary for a healthy organism. During reproduction, DNA from the parents gets carried over to the offspring. Changes in the structure and coding of DNA may therefore lead to a malfunctioning cell and have significant implications to the organism or its offspring.

Radiation can induce damage to DNA in two ways, namely via direct and indirect action [18]. In the first case, direct action, the ionizing radiation interacts directly with an atom of the DNA, thereby changing the structure or breaking a bond. The indirect activity acts through radiolysis of water, creating highly reactive hydrogen (H·) and hydroxyl radicals (OH·). These can on their turn interact with the DNA strand. Indirect activity accounts for about two thirds of the biological effects. Figure 2.10 gives an overview of the types of DNA-damage.

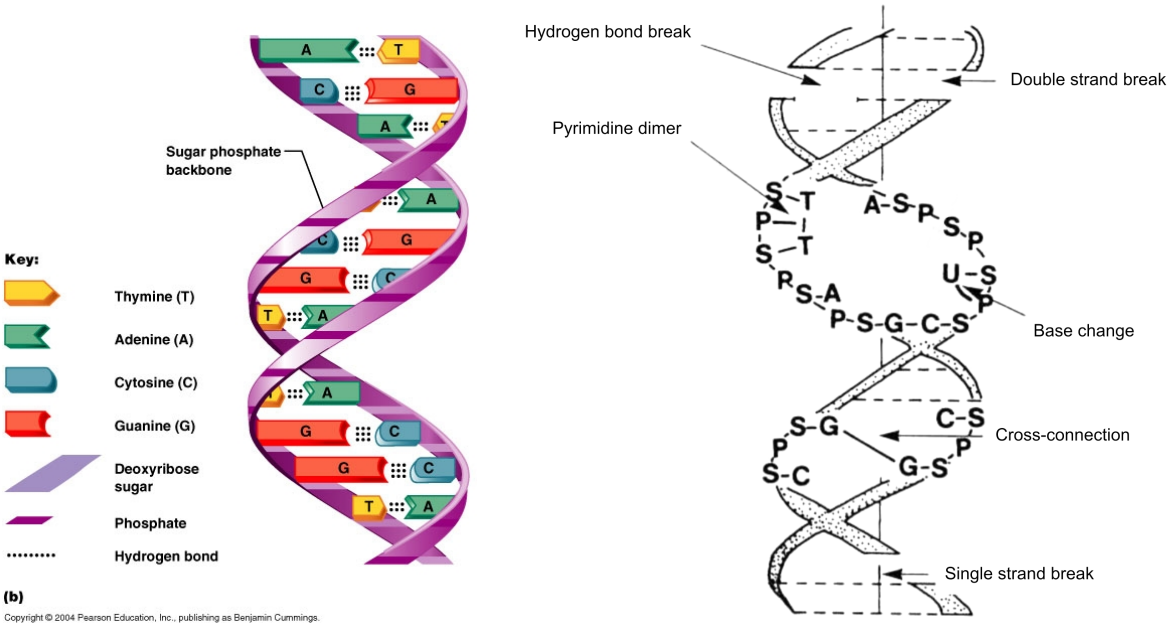

Figure 2.10: *Illustration of the structure of DNA and an overview of the types of DNA damage induced by ionizing radiation [29].*

Evolution has provided cells with mechanisms to repair the acquired damage. These mechanisms are however not 100% flawless and defects may be incorrectly repaired or not repaired at all. Out of all the damages the double strand break is the hardest to repair. There are three possible outcomes for the further life of the cell in such a case. First of all, there is still a possibility that the induced damage has no negative effect on the cell. The cell is still able to function without any anomalies. In the second case, the damage is too substantial and the cell cannot function properly, eventually leading to cell death. Exposure of a person to a high intensity of ionizing radiation can therefore result in large scale cell death, which may eventually lead to loss of organ function. Specifically for germ cells this would imply sterilization. These forms of biological effects are called deterministic effects and are typically only expressed above a case specific threshold dose as the number of cell kills is the determining factor. Once above the threshold, the severity of the effect increases as the dose is further increased. The skin, for example, develops redness (erythema) and hair loss when exceeding about 3-8 Gy (absorbed dose, see section 2.4) [30]. Different organs and structures have different radio-sensitivities. Factors such as the proliferation state, the structural composition and oxygen supply of the tissue affect the sensitivity. The last possibility involves a damaged cell which is still able to survive, but with some altered functionality. It are these mutations that can eventually lead to the formation of cancer or genetic defects carried over to offspring. Contrary to deterministic effects, it is believed that these mutations can occur at any received dose and are therefore called stochastic effects. It is however not always evident to link the cause of cancer or genetic defects to ionizing radiation. This is especially the case for small doses as many other factors can increase the probability of developing cancer, e.g. diet and smoking. Out of precaution a model without threshold is often assumed. This is the Linear No Threshold model, for which the chance to exhibit an effect due to irradiation is proportional with the received dose. Figure 2.11 illustrates this dependence

for both the stochastic and deterministic effects. The response of the human body on ionizing radiation does not only depend strictly on the absorbed dose. For each person the response will vary slightly. This individual susceptibility arises from differences in age, gender, diet, genetics, etc. This is also depicted in the graph for deterministic effects. It is due to this individual susceptibility that the frequency of deterministic effects is not a step function at a specific threshold dose, but slightly spread out.

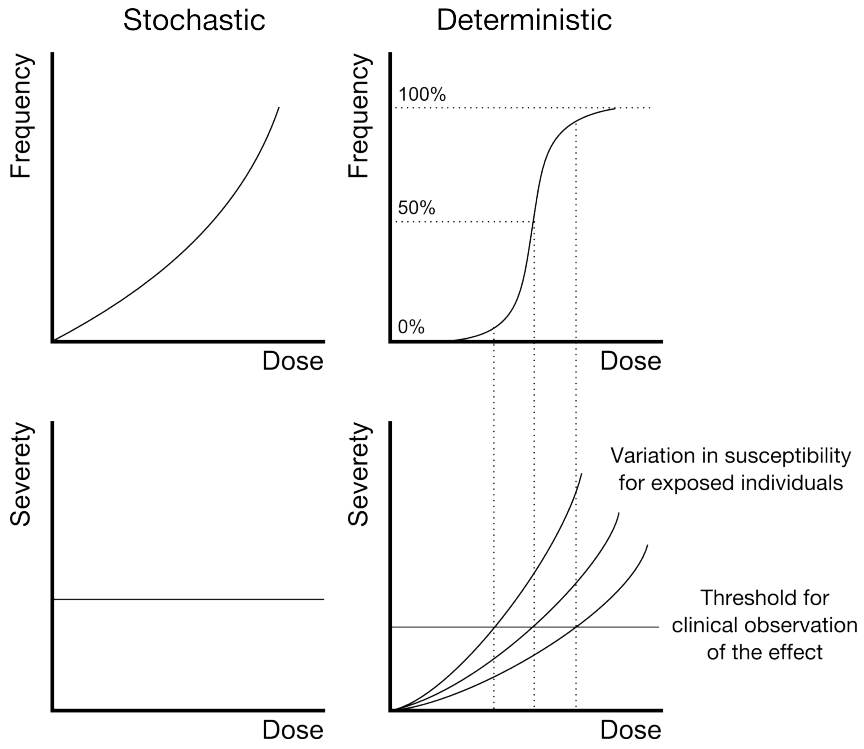

Figure 2.11: *Frequency and severety of stochastic and deterministic effects as a function of absorbed dose [30].*

An accidental exposure often involves irradiation of the whole body. When the total absorbed dose exceeds about 1 Gy, a series of symptoms will usually develop. This is called radiation sickness [31]. The first symptoms are nausea, vomiting, diarrhea, headache and fever, and arise after a few minutes to a few hours. The period between irradiation and the development of the symptoms varies depending on dose and exposure time. The higher the dose, the sooner they will manifest themselves. After this first wave of symptoms, a period in which no illness manifests itself may occur. However, after one to four weeks, new, more severe symptoms like hair loss, infections and low blood pressure may occur. If the total dose exceeds about 10 Gy, all these symptoms develop almost instantly and are often untreatable. Depending on the severity, the person dies within a couple days to weeks.

2.4 Radiation protection dose quantities

There is a need in radiation protection for a quantity which is a measure for the risk of exposure to ionizing radiation. Previous sections gave an overview of the interactions of ionizing radiation and the detrimental effects it may cause. The quantity thus needs to take into account the different radio-sensitivities of tissues and organs and the different responses for the types of ionizing radiation. The absorbed dose, D, is a pure physical quantity that does not include these factors [25, 32]. It however does form the basis for the wanted radiation protection quantities. The absorbed dose is defined as the mean absorbed energy per unit of mass, or

$$D = \frac{d\bar{\varepsilon}}{dm}. \qquad [Gy] \tag{2.16}$$

Here, $\bar{\varepsilon}$ denotes the mean absorbed energy, and m the mass of the surrounding region. The S.I. unit of absorbed dose is joule/kg. However, for this quantity a special name was introduced: the "gray" with symbol "Gy". We can transition from this physical quantity to a protection quantity by first of all taking the type of radiation into account. The types of radiation that produce a higher number of ionizations per unit length (Linear Energy Transfer, LET) are actually more harmful. The probability for radiation to interact with DNA and cause double strand breaks increases with increasing LET. Heavy charged particles have a higher LET than photons and electrons for example. The quantity that takes this into account is the equivalent dose H. Each type of radiation is assigned a radiation weighting factor, W_R, reflecting the LET. The value for each type is given in table 2.1 with exception of neutrons. Due to the strong energy dependence of the neutron interactions, a continuous energy dependent function is used instead of a fixed value. Figure 2.12 gives a graphical representation of the neutron radiation weighting factor. The equivalent dose in a certain tissue is then defined as

$$H_T = \sum_R W_R \; D_{R,T}. \qquad [Sv] \tag{2.17}$$

Here, $D_{R,T}$ is the average absorbed dose for a certain type of radiation (R) in some organ (T). The unit used for the equivalent dose is "Sievert', denoted with "Sv".

As mentioned in section 2.3, each organ reacts with a different intensity to an exposure. The effective dose, E, takes this into account by introducing a tissue weighting factor, and is defined as

$$E = \sum_T W_T H_T = \sum_T W_T \sum_R W_R D_{R,T}. \qquad [Sv] \tag{2.18}$$

The tissue weighting factors reflect the radio-sensitivity of the tissue. Table 2.2 gives an overview of the different values. The effective dose allows to compare all possible exposures (different organs, partial/whole body radiation) on one risk scale.

Radiation type	W_R
Photons	1
Electrons and muons	2
Protons and charged pions	20
Neutrons	See figure 2.12

Table 2.1: *Radiation weighting factors [32].*

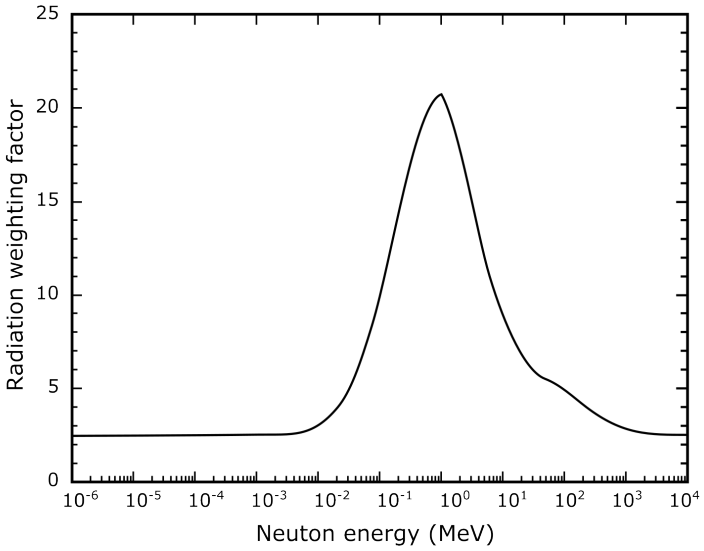

Figure 2.12: *Neutron radiation weighting factor W_R as a function of neutron energy [32].*

Tissue	W_T	$\sum W_T$
Bone marrow (red), colon, lungs, stomach, breast, remaining tissue	0.12	0.72
Gonads	0.08	0.08
Bladder, oesophagus, liver, thyroid	0.04	0.16
Bone surface, brain, salivary glands, skin	0.01	0.04
	Total	1.00

Table 2.2: *Tissue weighting factors [32].*

In practice however, these quantities are not used as they are not measurable due to their "biological" definition. As a consequence, operational quantities are used to evaluate the equivalent and effective dose in tissues. These quantities aim to give a conservative estimate of the protection quantities related to exposure of persons under most irradiation conditions. Different types of operational quantities are used for personal and ambient monitoring. The operational magnitude for individual monitoring is the individual dose equivalent $H_p(d)$, which is the dose equivalent in soft tissue at an appropriate depth d at a specified point in the human body. The specified point is normally the point where the individual dosimeter is worn. For the evaluation of the effective dose, $H_p(10)$ with a depth $d = 10\ mm$ is chosen, and for the evaluation of the dose to the skin and hands and feet the individual dose equivalent $H_p(0.07)$ at a depth $d = 0.07\ mm$ is used. The operational quantity for ambient monitoring is the ambient dose equivalent $H^*(10)$. It is thus

this quantity that is used throughout the simulations in this thesis. The ambient dose equivalent is the dose equivalent at a point in a radiation field that would be produced by a corresponding expanded and aligned field in a 30 cm diameter sphere of tissue of unit density at a depth of 10 mm, on the radius vector opposite to the direction of the aligned field [32, 33].

2.5 Regulation

To protect the population, and especially employees working with ionizing radiation, a legislation was constructed regarding the use and exposure to ionizing radiation. This legislation is built upon three primary principles, i.e. justification, optimization and personal dose limits [34]. The first principle, justification, enforces that any use of ionizing radiation must have a net positive effect on the exposed person, or on society. In the case of CERN MEDICIS, the exposure of employees does not have any positive consequences. In fact, the opposite is true. However, the medical purpose of the collected isotopes transcends this disadvantage. the principle of optimalization is based on keeping individual doses and the number of exposed individuals as low as reasonably achievable. This is the so called "ALARA" principle. A balance between radiation protection and the associated costs must therefore always be made for each application of ionizing radiation [35]. Some of the main principles of ALARA to reduce exposure are: reducing the time spent around a source, increasing your distance to the source, preventing internal contamination and adding shielding. For the personal dose limits, recommendations are established on a European level. These then need to be implemented by each of the member states in their legislation [34]. For CERN, the Swiss legislation is applicable [33]. The most important document concerning ionizing radiation in the Swiss law, is the 814.501 Radiological Protection Ordinance (RPO) [36]. It states that the maximal equivalent dose for an occupationally exposed individual is 20 mSv per year. In exceptional situations the employee may be allowed to exceed this value up to 50 mSv. The total equivalent dose over five consecutive years may however not exceed 100 mSv. Besides that, there are some extra dose limits for certain parts of the body. The equivalent dose to the eye lens is limited to 150 mSv per year. For the skin, hands and feet, the limit is set to 500 mSv per year. CERN must comply with these rules. An institution may however impose stricter conditions. This is the case at CERN, where they make a distinction between two categories of occupationally exposed persons. Category A comprises occupationally exposed persons that may be exposed to more than 3/10 of the limit in terms of effective dose in 12 consecutive months. Catergory B employees may not exceed 3/10 of the limit in 12 consecutive months [33]. CERN also distinguishes three types of areas depending on the level of hazard, i.e. non-designated areas, supervised radiation areas and controlled radiation areas. The equivalent dose limit for each area is respectively 1 mSv, 6 mSv and 20 mSv. To make sure that the area conforms to the limit in terms of the yearly equivalent dose, the limits are translated into an ambient dose equivalent rate, which can easily be measured. Table 2.3 gives an overview of the different areas together with the dose limits both in terms of equivalent dose and ambient dose equivalent rate. The right column shows which sign must be present at any entrance to the area.

	Area	Dose limit [year]	Ambient dose equivalent rate		Sign
			Work place	Low occupancy	
	Non-designated	1 mSv	0.5 µSv/h	2.5 µSv/h	
Radiation Area	Supervised	6 mSv	3 µSv/h	15 µSv/h	
	Simple	20 mSv	10 µSv/h	50 µSv/h	
	Limited Stay	20 mSv		2 mSv/h	
	High Radiation	20 mSv		100 mSv/h	
Controlled Area	Prohibited	20 mSv		> 100 mSv/h	

Table 2.3: *Synopsis of the classification of Non-designated Areas and Radiation Areas at CERN [33].*

In general, a distinction is made between sealed and unsealed sources. Sealed sources, need to comply to strong rules regarding the prevention of leaks. The radioactive substance is for example embedded into a leak resistant material or permanently sealed in a capsule [37]. Although the spread of any radioactive substances should be avoided, the sources at CERN MEDICIS will not conform to these specifications. Swiss legislation specifies three types of working areas for of unsealed radioactive sources, according to the activities handled per operation or per day:

- Type C: An activity from 1 to 100 times the licensing limit
- Type B: An activity from 1 to 10 000 times the licensing limit
- Type A: An activity from the licensing limit up to an upper limit that is defined in the licensing procedure.

The licensing limit (LA limit, Limite d'Authoristation) is specified in Annex 3 Column 10 of the Swiss RPO for most isotopes [36]. The definition of the limit is such that, if a person would inhale the LA activity of the specific isotope on a single occasion, the effective dose would equal 5 mSv. This classification should, however, not be confused with the classification from table 2.3. CERN MEDICIS is classified as a type A area as the activity of the medical grade unsealed sources is too high to conform to type B or C areas [6]. The upper limit is, however, not yet determined, as the procedure is in a state of negotiation. Besides, Swiss legislation states: "Work with unsealed radioactive sources whose activity exceeds the licensing limit specified in Annex 3 Column 10 must be carried out in working areas." [36]. Handling of the collected isotopes will be carried out in the experimental hall and is thus defined as a working area. In terms of CERN's own area classification, MEDICIS's experimental hall is a simple controlled area. Consequently, the limiting ambient dose equivalent rate is 10 μSv/h, as specified in table 2.3. This value is taken as the benchmark during the evaluation of all simulations.

Chapter 3

Discussion of the simulations

3.1 FLUKA

FLUKA, a Monte Carlo multi-particle transport code, is chosen to perform the simulations [38]. A first reason for this choice is that FLUKA is both used and developed at CERN. The code was specifically designed for dosimetric purposes and is extensively used in the design of accelerator shielding and target design, calorimetry, activation studies, etc. [39]. Working with FLUKA thus allows for a more compatible and efficient research workflow as MEDICIS is part of CERN. The implementation, refinement or adaptation of a model can then easily be carried out in subsequent work. The foundations of a model of the MEDICIS facility were already worked out by a previous student [40]. This model had to be refined, but proved to be a good starting point.

A user interface is provided under the name "Flair". This makes FLUKA a user friendly program for which, normally, no programming skills are required. So called "cards" are used to provide the necessary information of the model in an apprehensive way. They can be subdivided in multiple categories, in effect providing a structured code. The advantage of FLUKA is that the user does not need to have a profound knowledge about the models and the associated equations. One must however know about the physics such that the appropriate cards are included in the code. An example of one of the simulation performed can be found in appendix C. Complex geometries can be handled by FLUKA and are formed by means of combinatorial geometry. This means that complex shapes are made by adding and subtracting simpler shapes. Flair provides a graphical interface to see and debug the geometry. After a simulation, the obtained data files can directly be processed and plotted in Flair. It should be noted that when a two dimensional plot is made of a dose distribution, the dose is averaged over the third axis. It is possible to define boundaries over which the average is taken. This makes it possible to find areas of elevated dose which would otherwise be averaged away. The limits will be specified for every plot.

FLUKA is able to simulate the propagation and interaction of a large range of particles with great accuracy. The energy range for which FLUKA can simulate depends on the type of particle. Hadrons can be simulated for energies up to 20 TeV. For electrons and photons (including polarized and optical photons), the energy range ranges from 1 keV till a few thousand TeV. Muons and neutrinos can be simulated for any energy.

Neutrons, heavy ions and all the respective antiparticles down to thermal energies. The simulations carried out are thus perfectly possible in FLUKA as the energy values stay well within these ranges. More specifically the FLUKA manual specifies that a detailed generalized intra-nuclear cascade and pre-equilibrium stage model (see section 2.1) is used to calculate the interactions of hadrons with nuclear matter for energies up to 3-5 GeV. [39]

In a Monte Carlo code, like FLUKA, the transport is simulated by taking a number of initial particle histories. In FLUKA this number of histories is also known as "primaries". The transport is then performed in steps. At each step all possible interactions with the surrounding material are randomly sampled according to the probability of these interactions. Specifically in FLUKA, conservation laws are enforced and results are checked at each step as well [39]. In earlier Monte Carlo programs, the step length could drastically alter the results. FLUKA's algorithm, however, provides a robust independence of the result on the step length. This is mainly due to a more accurate determination of the path length correction, defined as the ratio between the length of the actual path of the particle and that of the straight step connecting the two endpoints [39]. When in the end, the particle comes to a stop, or reached the boundaries of the geometry, the code jumps to the next primary particle. This is done repeatedly until the user-defined amount of histories have been simulated. In this way the interactions of the protons impinging the MEDICIS target are simulated and new isotopes are created.

The decay of isotopes both in the target and at the collection point is managed in the simulations by the evaluation the direct solution of the Bateman Equations [39]. This set of first order differential equations forms a mathematical model describing abundances and activities in a decay chain as a function of time. An exact analytical solution is given by [41]:

$$N_n(t) = \sum_{i=1}^{n} \left[N_i(0) \times \left(\prod_{j=1}^{n-1} \right) \times \left(\sum_{j=1}^{n} \left(\frac{e^{-\lambda_j t}}{\prod_{p=i,p\neq j}^{n} (\lambda_p - \lambda_j)} \right) \right) \right]. \tag{3.1}$$

Here, $N_n(t)$ denotes the number of type n isotopes at a specific time t, with λ_i the decay constant for isotope i to decay to isotope $i+1$ [8]. In the end, so called "scoring cards" are used to define detectors which can estimate quantities like fluence, activity, deposited energy density, etc. As the main interest lies within area monitoring, the ambient dose equivalent is the quantity of interest (see section 2.4). FLUKA estimates this quantity by keeping track of the particle fluence in a user defined mesh in the region of interest. Afterwards, fluence to ambient dose equivalent conversion factors are used to obtain the requested quantity. FLUKA offers a range of conversion factors. The default setting is the "AMB74" set and was obtained from ICRP74 and Pelliccioni data [39, 42].

3.2 Incorporating the irradiated target

The collection point is located in the experimental hall and is, therefore, a first obvious source of radiation to employees. The target present in the separated area should, however, also be considered. The beamline passes trough a hole in the wall from the mass separator to the collection point. This opening is potentially a weak spot trough which radiation from the target may leak into the experimental hall. It is thus of great importance to assess the need of extra shielding as the dose limit of 10 μSv/h should not be exceeded. For the collection of ^{44}Sc, a titanium target is used. The UC_x target is, however, the limiting case in terms of radiotoxicity (see section 2.1) and is used instead.

3.2.1 UC_x target

The incorporation of the target in the simulation presents some difficulties. FLUKA is only able to simulate on-line activation of a target. In other words, the irradiation and decay of the produced products is simulated in the same geometry. This is, however, not representative for CERN MEDICIS, as the proton irradiation is carried out in the ISOLDE facility. To accomplish a realistic activation simulation in the MEDICIS facility, any unwanted interaction of the proton beam with the surrounding geometry should be prevented. Luckily, FLUKA offers the option to define a material that stops all of the primary particles (in this case the 1.4 GeV protons), while leaving all decay products untouched. The material settings for the target itself are taken to be UC_2 with a density of 7 g/m^3 [6]. To verify the concept, a simple simulation is carried out. The result can be seen in figure 3.1. The topmost figure shows the proton beam impinging the UC_x target. The beam clearly does not exit the sphere. The lower graph displays the ambient equivalent dose distribution in the vicinity of the target. The dose is indeed non-zero outside of the sphere, indicating that all decay particles were able to trespass.

The target is placed in the MEDICIS geometry provided from previous work and is irradiated for 18 hours with 1.4 GeV protons in the simulation. This value was chosen as the general irradiation time throughout the simulations and represents a worst case scenario. A one hour cooling is included to take transport, storage and preparation time into account. The results of the simulation are shown in figure 3.2. A feature that stands out immediately on the upper plot of figure 3.2, is the large amount of radiation in the experimental hall. Yet, the walls seem to have stopped all the radiation. The lower image clarifies the problem. A large section of the upper part of the wall is missing, creating an entrance for the radiation to the hall. Another important inaccuracy was the 8 cm lead shielding around the collection point. Internal communication provided information that this should instead be 10 cm thick steel. The flaws in the geometry were corrected according to the latest CAD drawings of the facility.

The results of the simulation in the adapted geometry are displayed in figure 3.3. It should be noted that, although the same irradiation conditions are used in figure 3.2 and 3.3, the dose around the target seems to be significantly higher in the later one. As explained in section 3.1, boundaries can be specified over which the obtained values are averaged in the third dimension. The boundaries in figure 3.3 are simply specified closer to the height of the target and the collection point(z=110 cm). The dose distribution in

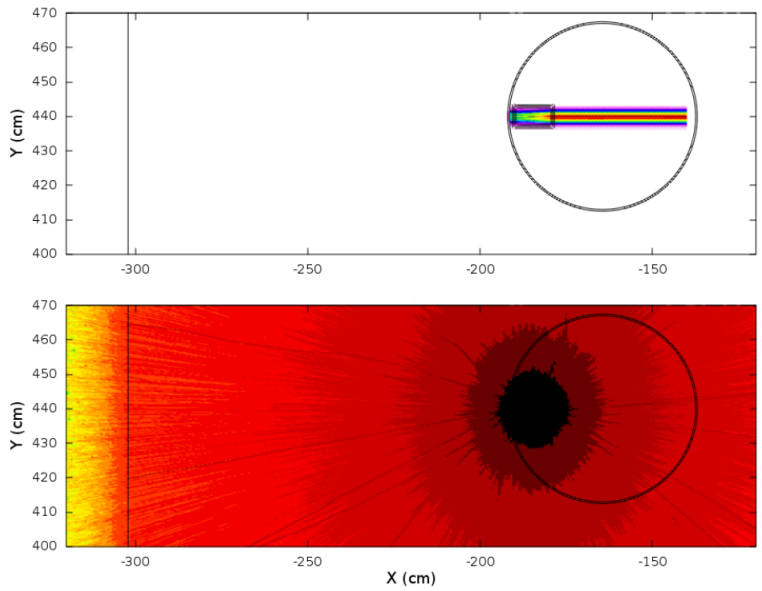

Figure 3.1: *Validation of the material settings in FLUKA for off-line target activation. Upper figure: Proton beam impinging the target, but does not leave the sphere. Lower figure: Dose distribution in the vicinity of the target proving that decay particles are able to go trough the sphere.*

the experimental hall differs significantly from previous simulation. Radiation is clearly leaking trough the opening in the wall. The lower graph of figure 3.3 shows a cross section of the distribution in the x-y plane right where the radiation leaves the shielding around the collection point. The radiation forms a circular hotspot a height of 110 cm and a diameter of ∼50 cm. For an average human, this is the height where the stomach, colon, gonads and other radiosensitive organs are located (see radiation weighting factors, section 2.4). Graph 3.4 denotes the value of the ambient dose equivalent along the beam of radiation in the experimental hall, starting from the shielding around the collection point. Right outside the collection point, the ambient dose equivalent equals about 100 μSv/h.

This is five times the allowed dose rate of 10 μSv/h, which is not acceptable in a work place. To prevent the leakage, extra shielding should be included. Therefore, a 65 cm high, 50 cm wide and 8 cm thick piece of shielding is added to the geometry. Its position is indicated in the middle plot of figure 3.5. The geometry and location is chosen such that it fully occludes the hole in the wall from the target. The thickness is derived from previous simulations. As mentioned before, the initial geometry incorporated 8 cm lead shielding around the collection point. As the change to 10 cm steel was discovered rather late, simulations of scandium collections were already performed. These proved that the 8 cm lead should provide the needed reduction in ambient dose rate. Figure 3.5 illustrates the result of 8 cm shielding in front of the opening. Ideally, the statistics in the experimental hall should be higher. This would, however, increase the simulation time to an unacceptable extent (∼ weeks). The amount of radiation entering the experimental hall is significantly reduced. The bottom figure demonstrates the effectiveness of the shielding as the circular hotspot is not observed any more. Additionally, the dose rate is below the threshold level of 10 μSv/h, as is indicated in figure 3.6.

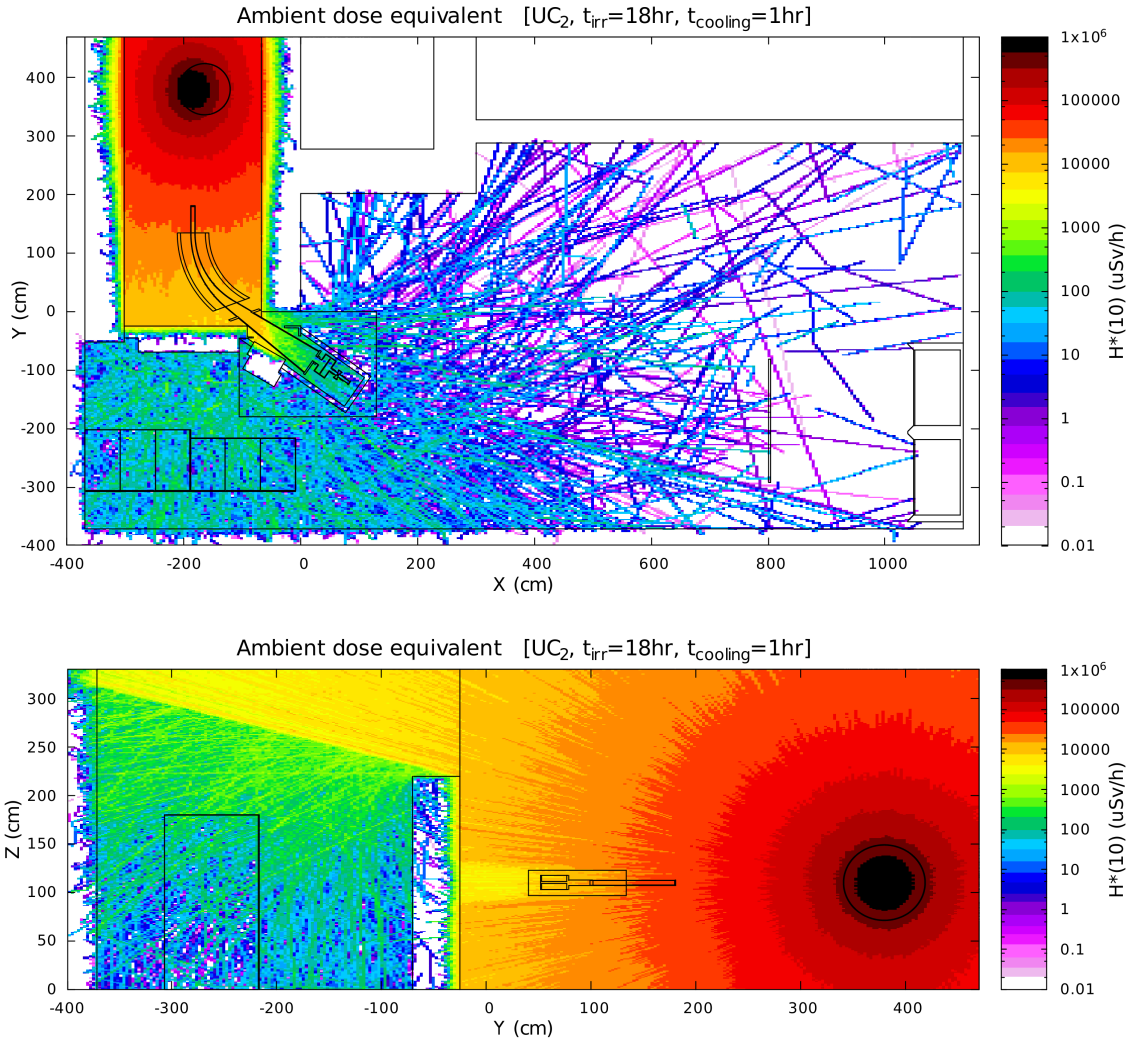

Figure 3.2: Top figure: *Top view of the ambient dose equivalent rate distribution, after 18 hour irradiation and 1 hour cooling of UC_2 target in the initial geometry (z-axis limits: [0 cm; 175 cm]).* Bottom figure: *Side view of the ambient dose equivalent distribution in the initial geometry (x-axis limits: [-300 cm; -90 cm]). [1.10^5 primaries]*

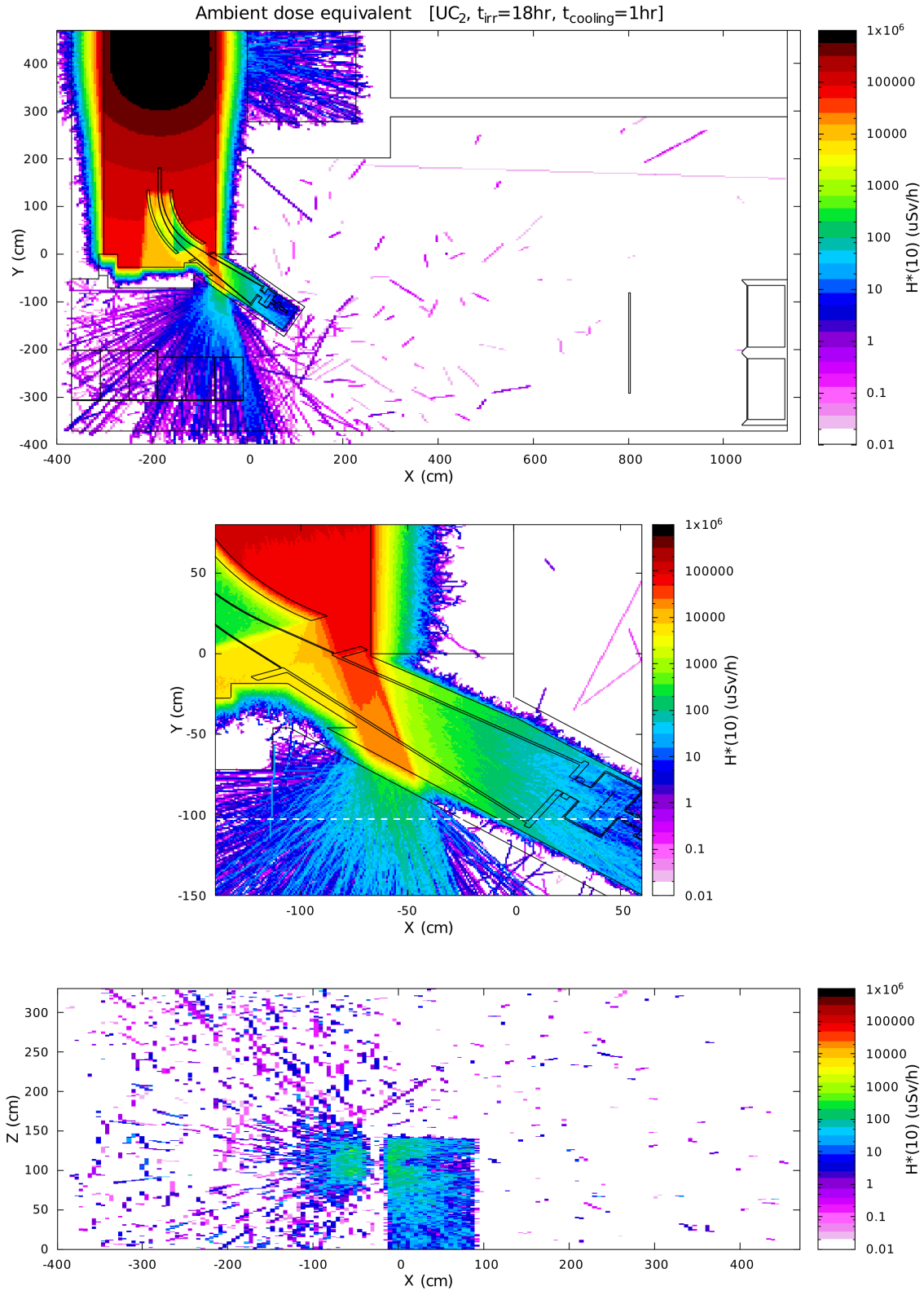

Figure 3.3: *The ambient dose equivalent rate distribution, after 18 hour irradiation and 1 hour cooling time of UC_2 target, in the adapted geometry.* Top figure: *Top view of the dose distribution (z-axis limits: [99 cm; 121 cm]).* Middle figure: *Detailed top view of the problematic area. The white dashed line indicates the position of the cross section taken in the bottom figure (z-axis limits: [99 cm; 121 cm]).* Bottom figure: *Side view of the dose distribution. The left circular hotspot originates from the leak. The rectangular shape originates from radiation inside the collection point's shielding (x-axis limits: [-101 cm; -98 cm]). [25.10^6 primaries]*

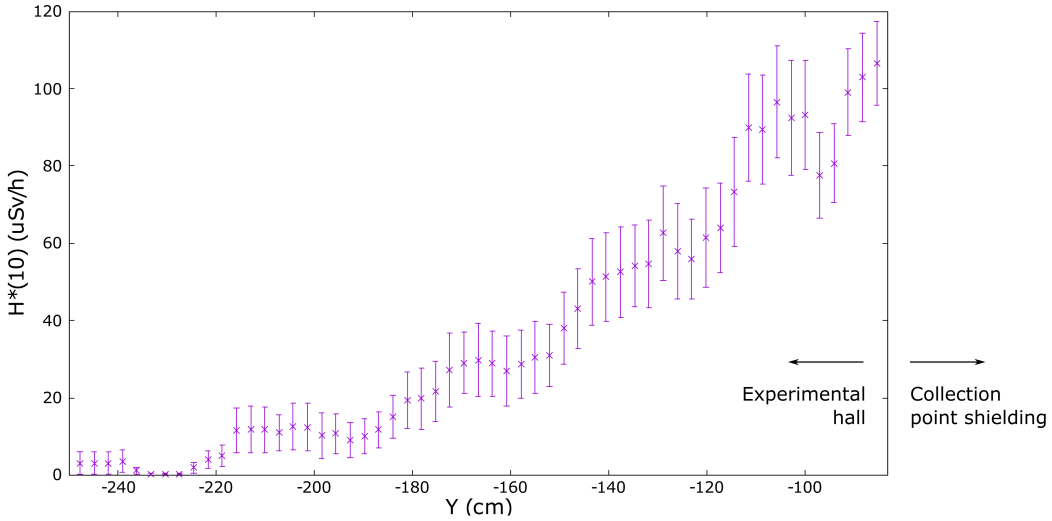

Figure 3.4: *Ambient dose equivalent rate along the beam of radiation entering the experimental hall for the UC_2 target. The rightmost boundary of the graph coincides with the shielding around the collection point (x-axis limits: [-58 cm; -48 cm], z-axis limits: [105 cm; 114 cm]).*

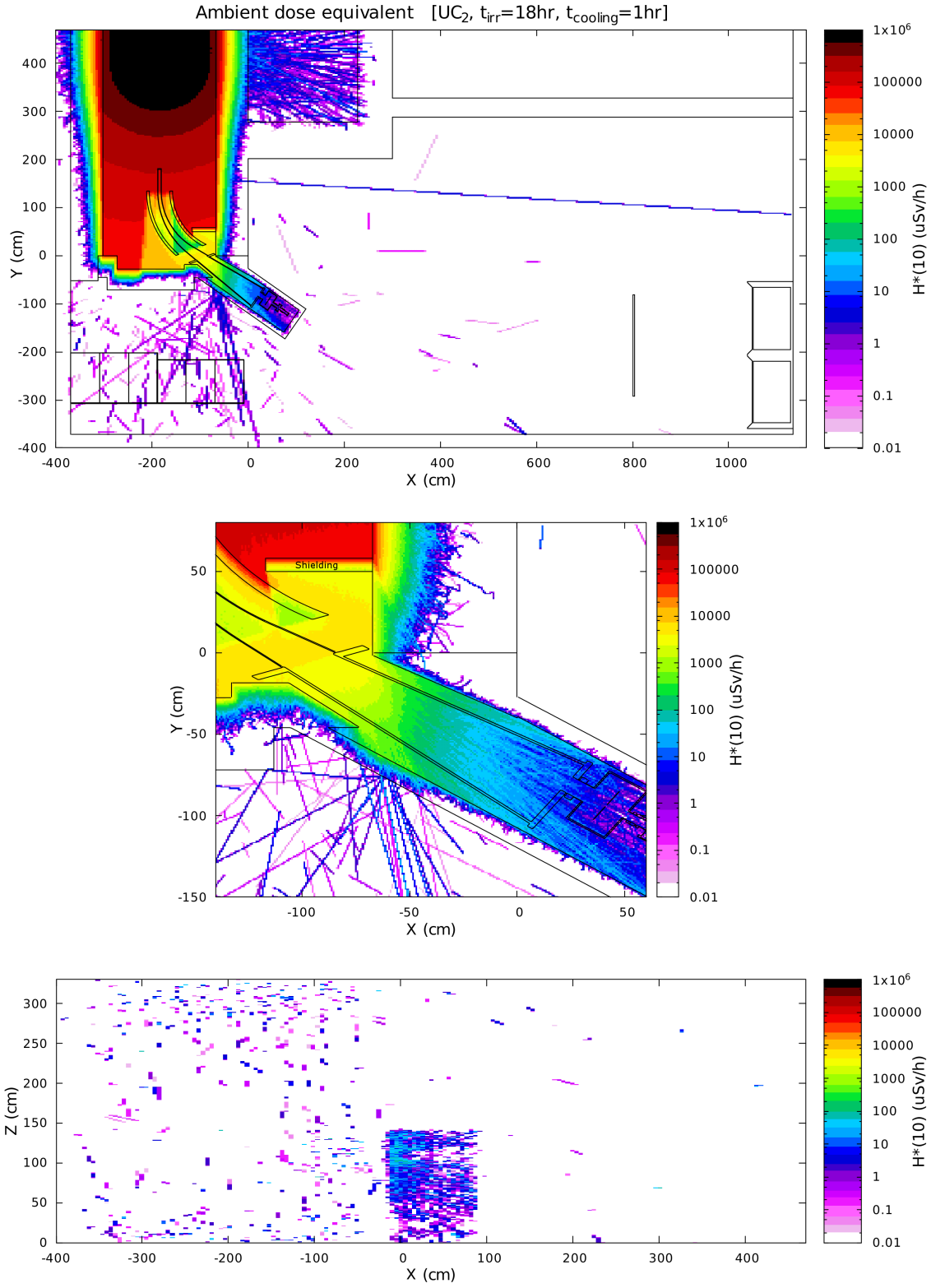

Figure 3.5: *The ambient dose equivalent rate distribution, after 18 hour irradiation and 1 hour cooling time of UC_2 target, with the additional shielding.* Top figure: *Top view of the dose distribution (z-axis limits: [99 cm; 121 cm]).* Middle figure: *Detailed top view of the problematic area. The added shielding is specifically indicated with "shielding". (z-axis limits: [99 cm; 121 cm]).* Bottom figure: *Side view of the dose distribution. The rectangular shape originates from radiation inside the collection point's shielding. (x-axis limits: [-101 cm; -98 cm]). [25.10^5 primaries]*

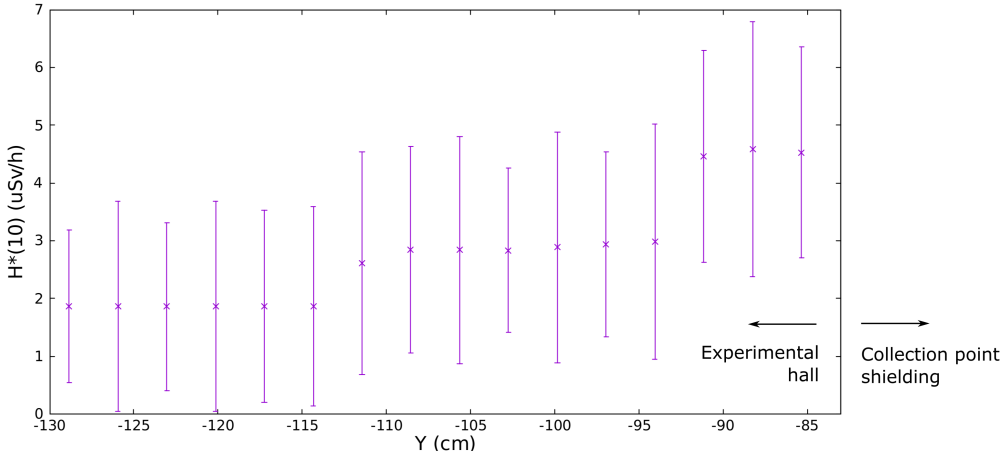

Figure 3.6: *Ambient dose equivalent rate along the beam of radiation entering the experimental hall for the UC_2 target, with the additional shielding. The rightmost boundary of the graph coincides with the shielding around the collection point (x-axis limits: [-68 cm; -53 cm], z-axis limits: [105 cm; 114 cm]).*

3.2.2 Ti target

As the collection of ^{44}Sc will make use of a titanium target instead of uranium carbide, a simulation with identical irradiation conditions is performed. The result is illustrated in figure 3.7. The ambient dose equivalent rate is, as expected, lower than for the uranium carbide target. As a consequence the shielding is also sufficient for the titanium target.

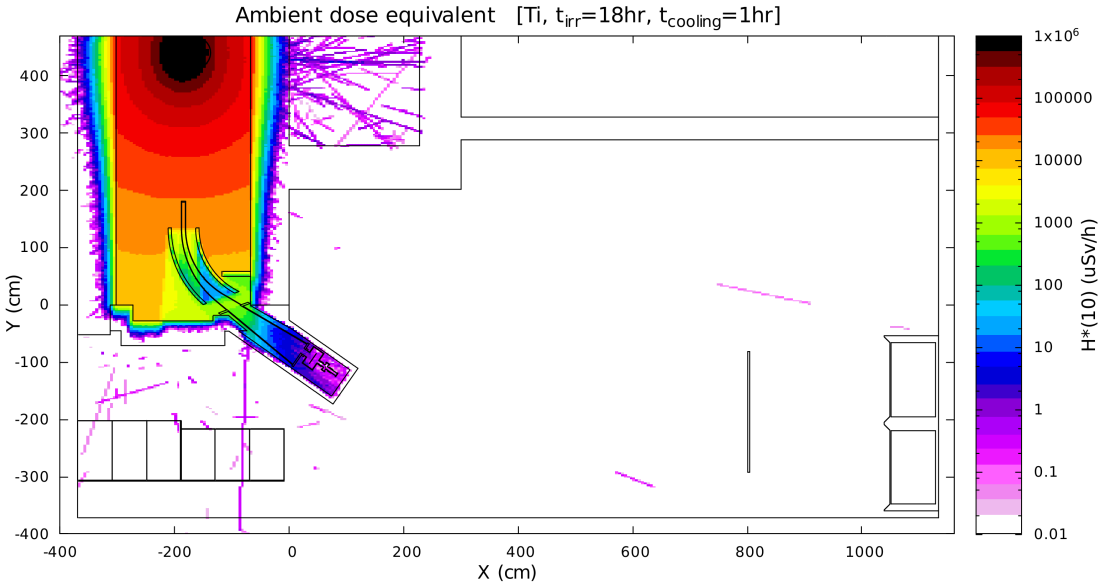

Figure 3.7: *Top view of the ambient dose equivalent rate distribution, after 18 hour irradiation and 1 hour cooling of the titanium target (z-axis limits: [99 cm; 121 cm]). [25.10^6 primaries]*

3.3 ^{44}Sc collection

To asses the effect of collecting ^{44}Sc on the dose distribution in the experimental hall, not only ^{44}Sc has to be taken into account. During the off-line mass separation, a whole array of scandium isotopes are sent trough the mass separator. Only ^{44}Sc reaches the collection point, while the others get caught by the walls or slits at the end of the separator (see figure 3.8). For the simulation, a selection of scandium isotopes is made according to their half lives. The first to be omitted is ^{45}Sc. ^{45}Sc is a stable element and does not contribute in any way to the dose. Scandium isotopes with atomic number smaller than 43 possess half-lives of the order of hundreds of milliseconds or less, as is shown in table 3.1. When taking the time for the target to be transported and prepared into account, it is safe to assume that these isotopes are reduced to negligible quantities. The same reasoning applies to the scandium isotopes with atomic mass number greater than 49. In case of ^{50}Sc, for example, the initial amount of nuclei is reduced by a factor 10^{11}, assuming the transport and preparation takes one hour. The half-life of the remaining isotopes are of the order of hours or days. Hence these will still be present in substantial quantities, as the half-lives are comparable or larger than the assumed one hour preparation time.

^{40}**Sc**	^{41}**Sc**	^{42}**Sc**	^{43}**Sc**	^{44}**Sc**	^{45}**Sc**	^{46}**Sc**
182.3 ms β^+	596.3 ms β^+	680.7 ms β^+	3.89 h β^+	3.97 h β^+	Stable /	83.79 d β^-
^{47}**Sc**	^{48}**Sc**	^{49}**Sc**	^{50}**Sc**	^{51}**Sc**	^{52}**Sc**	^{53}**Sc**
3.35 d β^-	43.67 h β^-	57.18 m β^-	102.5 s β^-	12.4 s β^-	200 ms β^-	2.4 s β^-

Table 3.1: *Half-life of scandium isotopes ($40 \leq A \leq 53$) and their main decay mode. [16]*

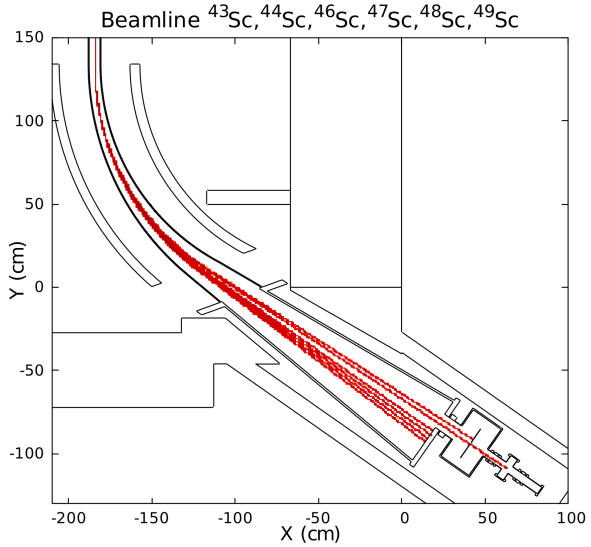

Figure 3.8: *The beam paths of the different radioactive scandium isotopes in the simulation. The beams from left to right coincide with ^{49}Sc till ^{43}Sc, respectively.*

A beam of each isotope is defined in the simulation, as is illustrated in figure 3.8. The collection time and beam current for the ^{44}Sc beam are chosen such that the accumulation results in 1.0 GBq at the collection point. Although table A.1 states that a collection of 2.9 GBq is expected, internal communication with CERN provided the information that a 1 GBq collection is sufficient for the end-users. The beam currents for the other isotope beams (^{43}Sc, ^{46}Sc, ^{47}Sc, ^{48}Sc and ^{49}Sc) are determined by the relative yields in the target. These values are extracted from the simulation in section 3.2.2 and are given in table 3.2. By increasing or decreasing the collection time, the collected activity can be changed accordingly in the simulation. Figure 3.9 illustrates the dose distribution, at the height of the collection point, immediately after a 1.0 GBq ^{44}Sc collection. The white dashed arrow in figure indicates the line along which the values shown in figure 3.10 are taken. Appendix B includes the results of a 2.9 GBq ^{44}Sc collection.

Isotope	**Absolute yield** ($\times 10^{14}$)	**relative yield**
^{43}Sc	19.49 ± 0.25	2.1%
^{44}Sc	46.89 ± 0.18	5.1%
^{46}Sc	386.79 ± 0.15	42.2%
^{47}Sc	407.01 ± 0.71	44.3%
^{48}Sc	46.25 ± 0.92	6.1%
^{49}Sc	0.92 ± 0.01	0.1%

Table 3.2: *Absolute and relative yield of the considered scandium isotopes in the titanium target after 18 hour irradiation and 1 hour cooling time according to the simulation.*

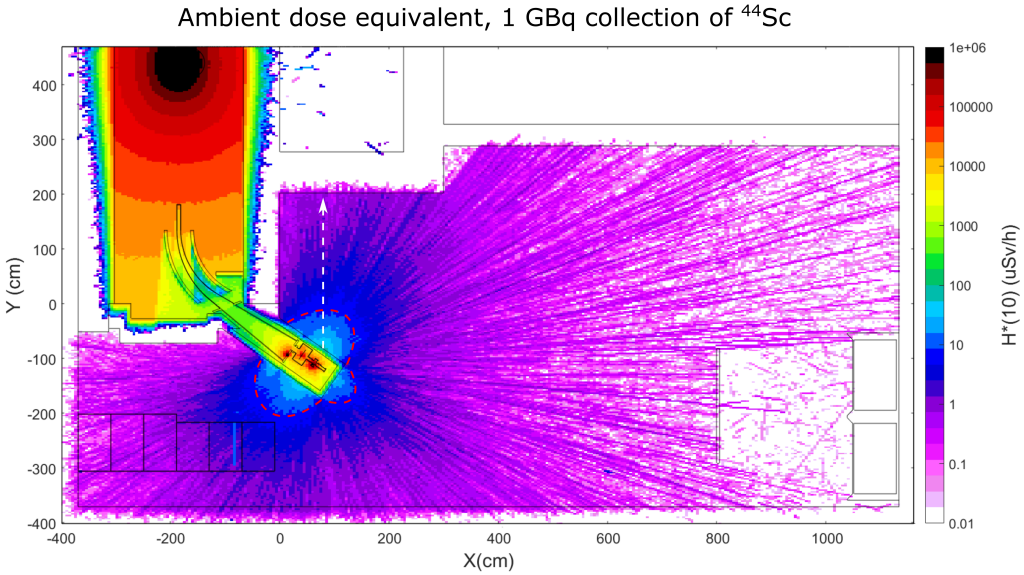

Figure 3.9: *Top view of the ambient dose equivalent rate distribution after a 1 GBq ^{44}Sc collection. The white dashed arrow in figure indicates the line along which the values shown in figure 3.10 are taken. The red dashed line indicates the area with a dose rate above 10 µSv/h. (z-axis limits: [99 cm; 121 cm]). [5.10^6 primaries]*

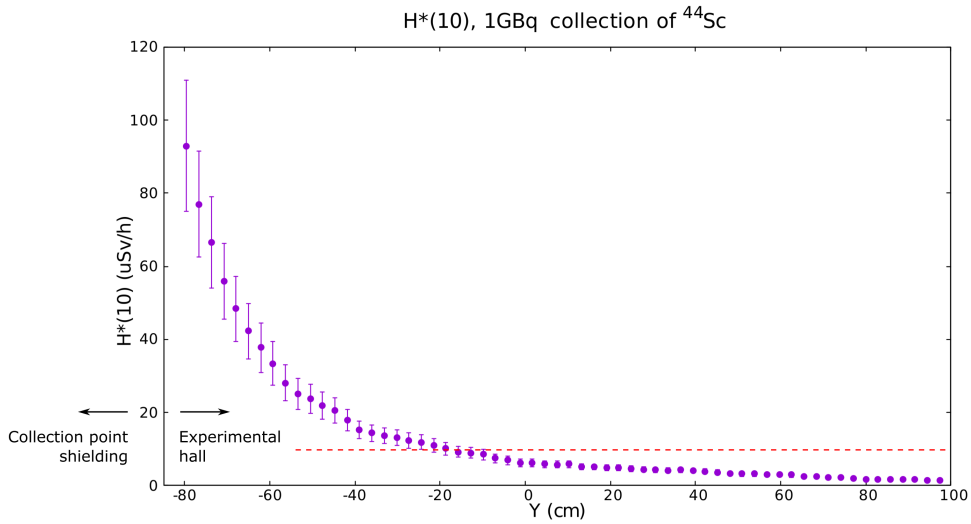

Figure 3.10: *The ambient dose equivalent rate along the white dashed arrow indicated in figure 3.9 after a 1 GBq ^{44}Sc collection. The leftmost axis coincides with the transition from the collection point's shielding to the experimental hall. The dose limit is indicated with a red dashed line.*

Figure 3.10 clearly shows, along with the color code in figure 3.9, that the ambient dose equivalent rate is higher than the dose limit of 10 μSv/h. More specifically, a minimal distance of 60 cm from the collection point is needed to reach a dose below the dose limit. This is however, not an option as the budget does not allow this. To solve this problem, two methods can be adopted. First of all, a physical barrier could be installed, preventing people from entering the high dose area in normal situations. The minimal area that should be demarcated is indicated in figure 3.9 by the red dashed line. This may however not be a practical solution as the demarcation would be positioned very close to the storage cabinet (bottom-left of the collection point) and thereby disrupt the passage way to the target area .

The other solution is to limit the collected activity such that the ambient dose equivalent rate does not exceed 10 μSv/h in the whole experimental hall. Figure 3.10 indicates that the highest dose rate is about 5 times the allowed limit. Therefore a 0.1 GBq collection is simulated. The results are shown in figure 3.11 and figure 3.12 in appendix **??**. The dose rate distribution is now lower than 10 μSv/h in the whole experimental hall. Right next to the collection point, the ambient dose equivalent coincides with the dose limit. The limiting activity during a ^{44}Sc collection is therefore 0.1 GBq.

Another apparent feature in the dose distribution in the hall is the significantly lower dose rate on the right side of the laboratory bench. This is due to the extra shielding provided by the lab bench. In general, it would thus be good good working principle to work on the right side of the bench. This is in line with the ALARA principle as it also increases the persons distance to the collection point.

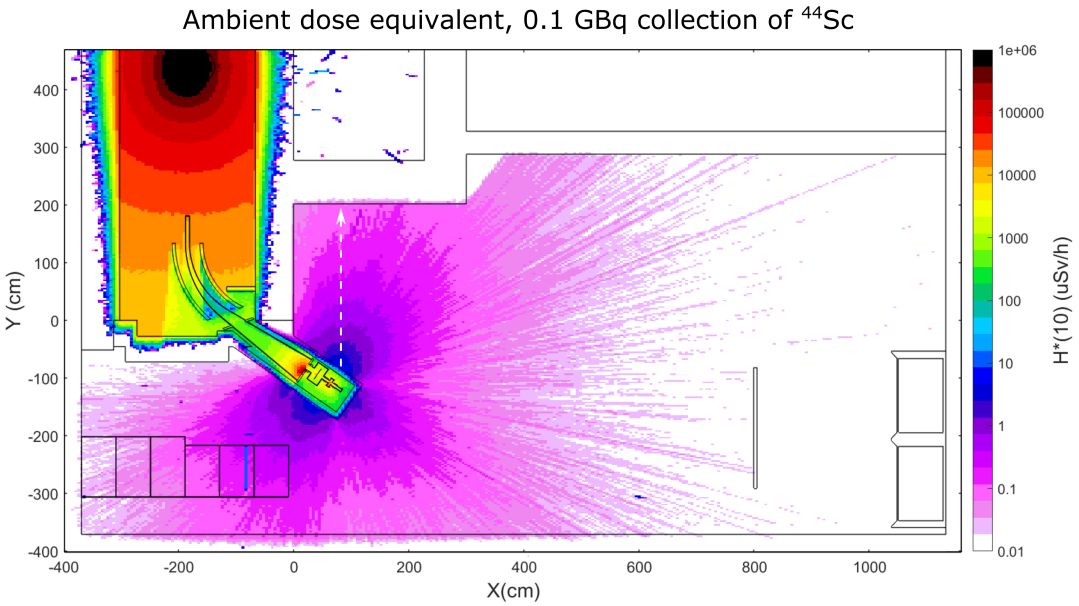

Figure 3.11: *Top view of the ambient dose equivalent rate distribution after a 0.1 GBq ^{44}Sc collection. The white dashed arrow in figure indicates the line along which the values shown in figure 3.12 are taken. The red dashed line indicates the area with a dose rate above 10 µSv/h. (z-axis limits: [99 cm; 121 cm]). [5.10^6 primaries]*

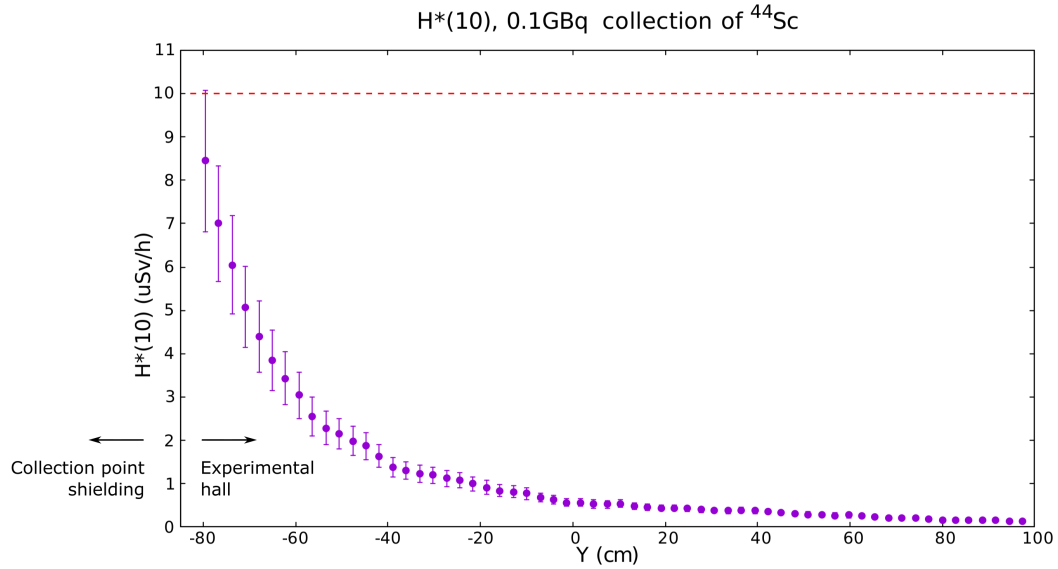

Figure 3.12: *The ambient dose equivalent rate along the white dashed arrow indicated in figure 3.11 after a 0.1 GBq ^{44}Sc collection. The leftmost axis coincides with the transition from the collection point's shielding to the experimental hall. The dose limit is indicated with a red dashed line.*

3.4 Accumulation of scandium isotopes on slits

During a batch collection of ^{44}Sc, the unwanted scandium isotopes are caught in the slits or the walls at the end of the separator (see figure 3.8). These parts are only replaced during maintenance after an operational year. Hence, a build up of activity may occur. As they are located in the experimental hall, they are able to contribute to the dose distribution. Moreover, precautions need to be made for the handling of the parts in case of high activities.

Assuming the daughter products are stable, as is the case for the considered scandium isotopes, the build-up is especially important for long lived isotopes (half-life $\sim$ months). Isotopes with half-lives in the order hours or days decay fast enough such that waiting a few days (depending on the half-life) is sufficient to significantly reduce the activity (see section 2.1.2). Regarding the collection of ^{44}Sc, ^{46}Sc is thus the most important isotope. With an half-life of 83.79 days, it has the longest half-life of all the scandium isotopes. The others have half-lives of at most a couple hours or days and are, therefore, not considered.

An operational year at CERN MEDICIS consists of 30 consecutive weeks [6]. The simulation, however, assumes one 1 GBq collection every day for 365 consecutive days. In this way the simulation represents a worst case scenario. The build-up of ^{46}Sc activity is calculated in the following way:

$$A_{build-up} = \sum_{d=1}^{365} A_0 . e^{\left(-\frac{\ln(2)d}{83.79 days}\right)}. \tag{3.2}$$

Here, A_0 denotes the ^{46}Sc activity after one collection. This value is obtained from the ^{44}Sc collection simulation and is equal to 35.74 MBq. Entering this value into the equation results in a build-up activity of 4.09 GBq after 365 days. A graphical representation of the build up of ^{46}Sc is given in figure 3.13.

The result of a simulation of a 4.09 GBq ^{46}Sc build up at the slits is shown in figure 3.13. The resulting ambient dose equivalent rate is smaller than 1 μSv/h in the whole experimental hall and should, therefore, not cause any issues.

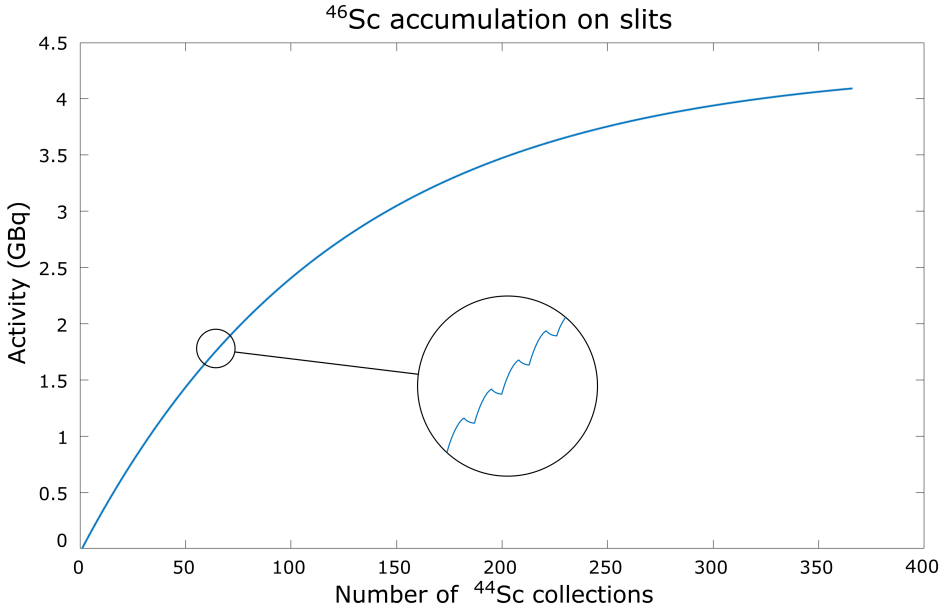

Figure 3.13: *The build-up of activity as a function of time for a daily collection of 35.74 MBq ^{46}Sc. The enlarged portion indicates the cycle of accumulation during collection and decay between collections.*

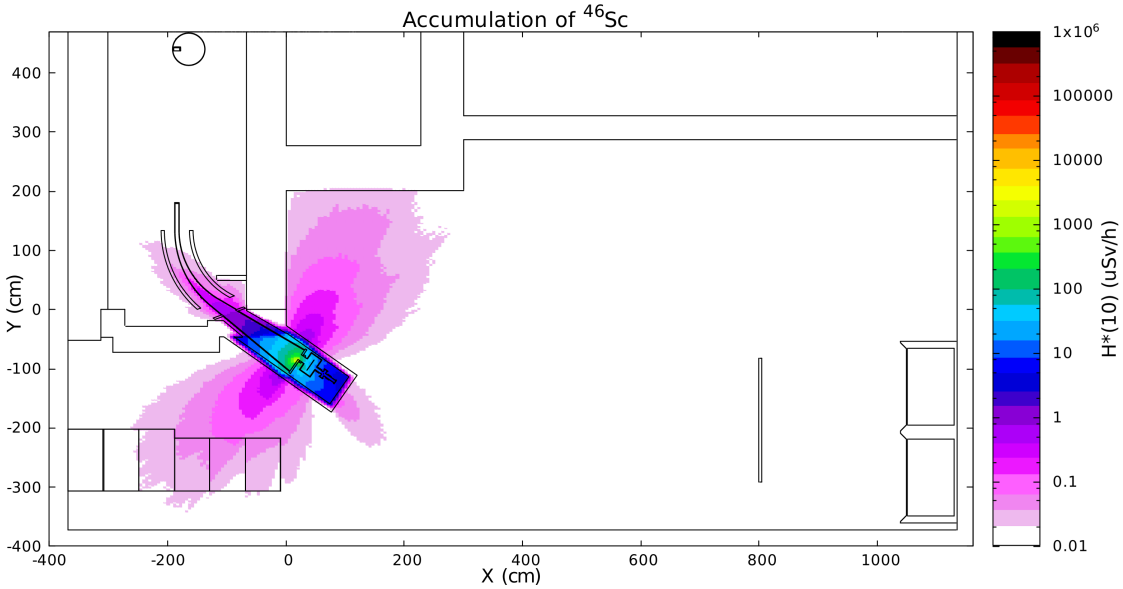

Figure 3.14: *Top view of the ambient dose equivalent rate distribution after a 4.09 GBq ^{46}Sc collection. (z-axis limits: [99 cm; 121 cm]). [5.10^6 primaries]*

Chapter 4

Conclusions and outlook

During the collection of ^{44}Sc, the target, the collection point and the slits, proved to contribute to the dose distribution in the experimental hall. The irradiated carbide target is this regard especially important. A hotspot of elevated dose is observed at a height of 110 cm, right where radio-sensitive organs are positioned in the human body. The simulations showed that at least 8 cm of shielding should be installed in front of the opening to sufficiently reduce the dose level and to make the hotspot disappear.

Simulations of the expected collection of 1 GBq ^{44}Sc, showed that the resulting dose distribution in the experimental hall exceeds the dose limit. The troublesome area is located within a distance of 40 cm of the collection point's shielding. Two solutions may be adopted. A physical barrier can be included such that employees are not able to enter the area where the dose limit is exceeded. This may, however, not be a practical solution as the available space is limited. The storage rack would be positioned close to the demarcation, thereby, blocking the passage way to the target area. As an alternative, smaller batches can be collected such that the dose limit is not exceeded in the whole experimental hall. The simulations showed that a 0.1 GBq ^{44}Sc collection would then be the limiting case.

The accumulation of activity on the slits and walls is mainly defined by ^{46}Sc due to its long half-life. A full year of collecting 1 GBq ^{44}Sc results in an accumulated activity of 4 GBq ^{46}Sc on the slits. The associated dose distribution in the experimental hall is below 1 μSv/h. This is well below the specified dose limit and should not cause complications during normal operation.

In addition to the considered scandium isotopes in the simulation, contaminations could be included. Surface ionizations in the ion source can cause other elements to reach the separator and, thereby, possibly contribute to the dose in the experimental hall. As mentioned before, this form of ionization is mainly a problem for alkali and earth alkali metals. The main contaminations during a scandium collection would therefore be calcium an potassium isotopes. Furthermore, sources of radiation could be positioned in the glove box, on the lab bench, etc. In this way the post-processing of the target can be simulated. Finally, the simulations should be validated by making measurements in the facility during the different situations.

Bibliography

[1] CERN. The ISOLDE the Radioactive Ion Beam facility, n.d. URL `http://isolde.web.cern.ch`. Retrieved: 2/08/17.

[2] CERN. The Proton Synchrotron Booster, 2017. URL `https://home.cern/about/accelerators/proton-synchrotron-booster`. Retrieved: 2/08/17.

[3] Nörtershäuser W. Recent developments in collinear laser spectroscopy at COLLAPS/ISOLDE. *Hyperfine Interactions*, 198(1):73–83, Jun 2010.

[4] Procter T. J. and Flanagan K. T. First on-line results from the CRIS (Collinear Resonant Ionisation Spectroscopy) beam line at ISOLDE. *Hyperfine Interactions*, 216(1):89–93, Apr 2013.

[5] G. Benzoni et al. Isolde Decay Station - IDS. Technical Report CERN-INTC-2015-009. INTC-SR-046, CERN, Geneva, Jan 2015.

[6] dos Santos Augusto R.M., Buehler L., Lawson Z., Marzari S., Stachura M., Stora T., and CERN-MEDICIS collaboration. CERN-MEDICIS (Medical Isotopes Collected from ISOLDE): A New Facility. *Applied Sciences*, 4(2):265–281, 2014.

[7] Morley T.J., Dodd M., Gagnon K., Hanemaayer V., Wilson J., McQuarrie S.A., English W., Ruth T.J., Bnard F., and Schaffer P. An automated module for the separation and purification of cyclotron-produced 99mTcO4. *Nuclear Medicine and Biology*, 39(4):551 – 559, 2012.

[8] Brown A. Design of the CERN MEDICIS Collection and Sample Extraction System, 2015. CERN thesis, 2015-251.

[9] Benlliure J. *Spallation Reactions in Applied and Fundamental Research*, pages 191–238. Springer Berlin Heidelberg, 2006.

[10] Kraan A.C. Range Verification Methods in Particle Therapy: Underlying Physics and Monte Carlo Modeling. *Frontiers in Oncology*, 5:150, 2015.

[11] Krása A. Spallation Reaction Physics, May 2010.

[12] Loveland W.D., Morrissey D.J., and Seaborg G.T. *Modern Nuclear Chemistry*. Wiley, 2 edition, 2017.

[13] Zeman J. Reactor Physics I., 2003. CVUT.

[14] Miller J.M. and Hudis J. High-Energy Nuclear Reactions. *Annual Review of Nuclear Science*, 9(1):159–202, 1959.

[15] Armbruster et al. P. Measurement of a Complete Set of Nuclides, Cross Sections, and Kinetic Energies in Spallation of ^{238}U $1A$ GeV with Protons. *Phys. Rev. Lett.*, 93: 212701, Nov 2004.

[16] National Nuclear Data Centre. Chart of Nuclides, n.d. URL `http://www.nndc.bnl.gov/`. retrieved: 21/05/17.

[17] Knoll G.F. *Radiation Detection and Measurement*. John Wiley & Sons, fourth edition, 2010.

[18] Cember H. and Johnson T.E. *Introduction to Health Physics*. McGraw-Hill, Health Professions Division, 1996.

[19] Nave C.R. Threshhold for relativistic effects. Online, 2017. URL `http://hyperphysics.phy-astr.gsu.edu/hbase/Relativ/rellim.html`. Retrieved: 22/05/17.

[20] Bogaerts R. Radiation Protection: general aspects. presentation, September 2016. course: Radiation Protection.

[21] The NIST reference on Constants, Units and Uncertainty. proton-electron mass-ratio. Online, 2014. URL `http://physics.nist.gov/cgi-bin/cuu/Value?mpsme`. Retrieved: 10/05/17.

[22] Ziegler J.F. The Stopping and Ranges of Ions in Matter, 1980.

[23] Thompson et. al A. X-RAY DATA BOOKLET, 2009.

[24] Sauli F. *Interaction of photons and neutrons with matter*. Cambridge Monographs on Particle Physics, Nuclear Physics and Cosmology. Cambridge University Press, 2014.

[25] Bos A.J.J. *Inleiding tot de stralingshygiëne*. Elsevier gezondheidszorg, 2000.

[26] Kaye & Laby Tables of Physical & Chemical Constants. Neutron Cross-sections, 2012. URL `http://www.kayelaby.npl.co.uk/atomic_and_nuclear_physics/4_7/4_7_2.html`. Retrieved: 1/06/17.

[27] Nuclear Power for Everybody. Cadmium 113 edge. Online, 2016. URL `http://www.nuclear-power.net/glossary/cadmium/cadmium-113-edge/`. Retrieved: 19/05/17.

[28] Peterson O.H., editor. *Lecture Notes: Human Physiology*. John Wiley and Sons Ltd, fifth edition, 2006.

[29] Silverthorn D.U. Human Physiology: An Integrated Approach, 2015. Pearson Education.

[30] ICRP. ICRP Statement on Tissue Reactions / Early and Late Effects of Radiation in Normal Tissues and Organs Threshold Doses for Tissue Reactions in a Radiation Protection Context. ICRP Publication 118. Ann. ICRP 41(1/2)., 2012.

[31] Mayo Foundation for Medical Education and Research. Radiation sickness, 2015. URL `http://www.mayoclinic.org/diseases-conditions/radiation-sickness/basics/symptoms/con-20022901`. Retrieved: 8/08/17.

[32] ICRP. The 2007 Recommendations of the International Commission on Radiological Protection. ICRP Publication 103. Ann. ICRP 37 (2-4)., 2007.

[33] Forkel-Wirth D., Roesler S., Silari M., M. Streit-Bianchi, Theis C., and Vincke H. Radiation protection at CERN. Technical report, CERN, 2011.

[34] Vanmarcke H. Stralingsbescherming Deel II, February 2017.

[35] CERN. CODE DE SéCURITé SAFETY CODE Mandatory as defined in SAPOCO/42, November 2006. F Rev.

[36] The Swiss Federal Council. Radiological Protection Ordinance (RPO) of 22 June 1994. Status as of 1 January 2014.

[37] International Atomic Energy Agency. Waste Technology Section, June 2016. URL `https://www.iaea.org/OurWork/ST/NE/NEFW/Technical-Areas/WTS/sealedsources-sealedsources.html`. Retrieved: 15/08/17.

[38] Böhlen T.T., Cerutti F., Chin M.P.W., Fassò A., Ferrari A., Ortega P.G., Mairani A., Sala P.R., Smirnov G., and Vlachoudis V. The FLUKA Code: Developments and Challenges for High Energy and Medical Applications. *Nuclear Data Sheets*, 120:211–214, June 2014.

[39] Ferrari A., Sala P.R., Fassò A., and Ranft J. *FLUKA: a multi-particle transport code.* CERN, 2011.

[40] Srakaew K. Validation and testing of the collection chambers for the CERN-MEDICIS project, 2016.

[41] Bateman H. Solution of a system of differential equations occurring in the theory of radioactive transformations. Proc. Cambridge Phil. Soc. IS, 423 (1910).

[42] Pelliccioni M. Overview of Fluence-to-Effective Dose and Fluence-to-Ambient Dose Equivalent Conversion Coefficients for High Energy Radiation Calculated Using the FLUKA Code. *Radiation Protection Dosimetry*, 88(4):279–297, 2000.

[43] ICRU. Report 49: Stopping Powers and Ranges for Protons and Alpha Particles, 1993. Report 49.

Appendix A

Isotopes to be collected

Medical Application	Isotope half-life	Parent isotope beam	Target ion source	CERN-MEDICIS		Comments
				In-target Activity (Bq)	Extracted Activity (Bq)	
α,β therapy/ SPECT/	^{213}Bi 45.6 m	^{225}Ac	UC_X-Re	2.8 E8	2.8 E7	Only mass separation
α,β therapy	^{212}Bi 60.6 m	^{224}Ac	UC_X-Re	1.7 E9	1.7 E8	Only mass separation
β therapy	*^{177}Lu 6.7 d*	*^{177}Lu RILIS/VD*	*Ta-Re/ Re-VD5*	*6.4 E8*	*6.4 E6*	*Chemical purification*
Auger therapy	^{166}Yb 56.7 h	^{166}Yb	Ta-Re	4.1 E10	2.1 E9	Chemical purification
β therapy	*^{166}Ho 25.8 h*	*^{166}Ho*	*Ta-Re*	*9.6 E6*	*4.8 E5*	*Chemical purification*
β therapy /Auger therapy	*^{161}Tb 6.9 d*	*^{161}Tb*	*UC_X-Re*	*1.9 E7*	*9.5 E5*	*Chemical purification*
PET	*^{156}Tb 5.35 d*	*^{156}Tb*	*Ta-Re*	*5.5 E7*	*5.5 E5*	*Chemical purification*
SPECT/ CT diagnosis	^{155}Tb 5.33 d	^{155}Dy/ Tb	Ta-Re	5.3 E9	5.3 E7	RILIS Dy
β therapy	^{153}Sm 46.8 h	^{153}Sm	UC_X-Re	2.8 E9	1.4 E8	Chemical purification
PET/CT	^{152}Tb 17.5 h	^{152}Dy/ Tb	Ta-Re	3.7 E10	3.7 E8	RILIS Dy
α therapy	^{149}Tb 4.1 h	^{149}Tb	Ta-Re	3.8 E10	3.8 E8	Chemical purification
^{140}Pr-PET/ Auger therapy	^{140}Nd 3.4 d	^{140}Nd	Ta-Re	1.2 E10	6.0 E8	Chemical purification

Medical Application	Isotope half-life	Parent isotope beam	Target ion source	CERN-MEDICIS		Comments
				In-target Activity (Bq)	Extracted Activity (Bq)	
β therapy	^{89}Sr 50.5 d	^{89}Sr	UC_X-Re	2.0 E9	1.0 E8	Only mass separation
PET	^{82}Sr 25.5 d	^{82}Sr	UC_X-Re	1.7 E9	8.5 E7	Only mass separation
β therapy	^{77}As 38.8 h	^{77}As	UC_X-VD5	5.8 E9	2.9 E8	Chemical purification
PET	^{74}As 17.8 d	^{74}As	Y_2O_3 -VD5	3.8 E8	1.9 E7	Chemical purification
PET	^{72}As 26.0 d	^{72}As	Y_2O_3-VD5	9.1 E9	4.6 E8	Chemical purification
PET	^{71}As 65.3 h	^{71}As	Y_2O_3-VD5	5.9 E9	3.0 E8	Chemical purification
β therapy	^{67}Cu 61.9 h	^{67}Cu	UC_X-Re	1.5 E9	1.1 E8	Chemical purification
PET, dosimetry, therapy	^{64}Cu 12.7 h	^{64}Cu	Y_2O_3-VD5	7.1 E9	3.6 E8	Chemical purification
PET	^{61}Cu 3.3 h	^{61}Cu	Y_2O_3-VD5	5.1 E9	2.6 E8	Only mass separation
β therapy	^{47}Sc 3.4 d	^{47}Sc	Ti	4.2 E10	2.1 E9	Evaporation
PET	^{44}Sc 4.0 h	^{44}Sc	Ti	5.7 E10	2.9 E9	Evaporation
PET	^{11}C 20.3 m	^{11}CO	NaF-LiF-VD5 ◊	-	1.4 E9	Only mass separation

Table A.1: *Isotopes to be collected at CERN MEDICIS. Table reproduced from [6].*

Appendix B

2.9 GBq ^{44}Sc collection

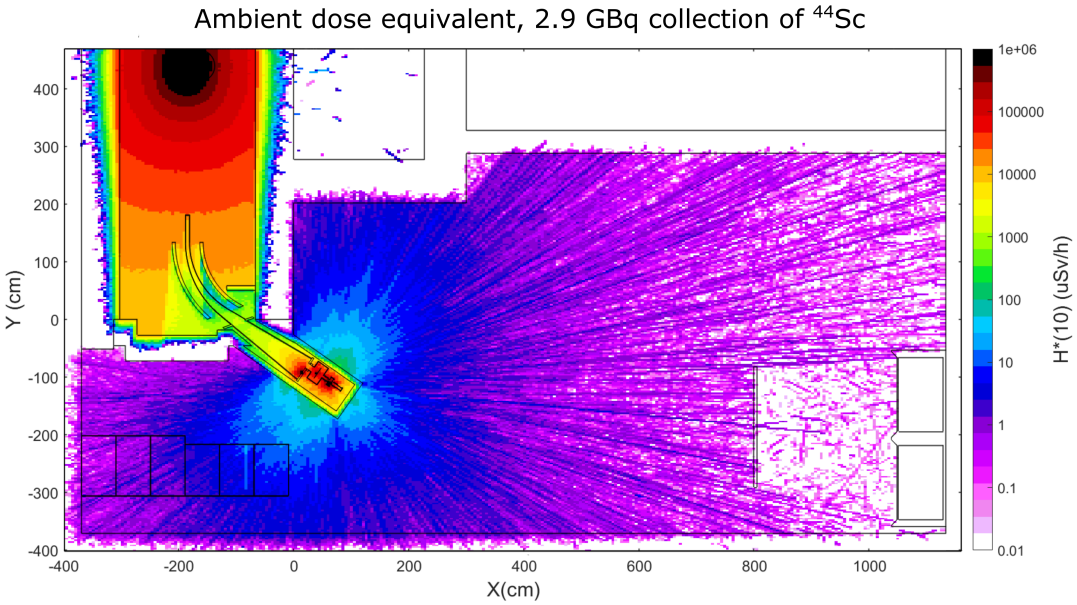

Figure B.1: *Top view of the ambient dose equivalent rate distribution after a 2.9 GBq ^{44}Sc collection. (z-axis limits: [99cm; 121cm]). [5E6 primaries]*

Appendix C

FLUKA code: Ti target irradiation

```
TITLE
MEDICIS simulation
* Set the defaults for precision simulations
DEFAULTS                                                              PRECISIO
*
* 1.4GeV Proton irradiation of the target
*
BEAM             -1.4                                -1.5       -1.5      PROTON
BEAMPOS         440.0      110.0     -140.0          0.0        0.0      NEGATIVE
*
* 2.0GeV Proton irradiation of the target
* !don't forget to change Irrprofi p/s!
*
*BEAM             -2.0                           -0.82425   -0.82425      PROTON
*BEAMPOS          380.       110.      -140.         0.0        0.0      NEGATIVE
*
* Mass separation isotope beam
* AFTER LASER SELECTION
*
*BEAM        -2.013E-7       -0.0      -0.0                               HEAVYION
*BEAMPOS         170.0      110.0     -184.0        -1.0        0.0
*HI-PROPE         65.0      149.0
ROT-DEFI         200.        0.0       30.0-39.406388        0.0 60.933358doortrans
ROT-DEFI         200.        0.0       35.0-52.522013      110.0114.080012rot35
PHYSICS            3.                                                 EVAPORAT
PHYSICS            3.0                                                COALESCE
PHYSICS            1.                          3-HELIUM   @LASTPAR    DECAYS
PHYSICS            1.          1.                                     IONBRPAI
IONFLUCT           1.          1.          4.  BLCKHOLE   @LASTMAT
PHYSICS            1.                                                 IONSPLIT
GEOBEGIN                                                              COMBNAME
    0    0
*
* ----------------------------------------------------------------------
* >>Room<<
* ----------------------------------------------------------------------
RPP blkbody     -407.0 475.0 -25.0 349.0 -404.0 1166.0
RPP wall        -402.0 470.0 -20.0 344.0 -399.0 1161.0
RPP air         -372.0 470.0 0.0 330.0 -369.0 1134.0
* Heavy wall
* ......................................................................
RPP hwall1      288.0 328.0 0.0 330.0 300.0 1134.0
RPP hwall2      202.0 277.0 0.0 330.0 0.0 300.0
RPP hwall3      277.0 470.0 0.0 330.0 227.0 300.0
RPP hwall4      0.0 470.0 0.0 330.0 -67.0 0.0
RPP hwall5      -52.0 470.0 0.0 330.0 -369.0 -302.0
RPP hwall6      -52.0 0.0 0.0 330.0 -312.5 -302.0
YZP O1          -3.0
YZP O2          -6.0
YZP O3          -9.0
YZP O4          -12.0
```

```
YZP O5          -15.0
YZP O6          -18.0
YZP O7          -21.0
YZP O8          -24.0
YZP O9          -27.0
YZP O10         -30.0
YZP O11         -33.0
YZP O12         -36.0
YZP O13         -39.0
YZP O14         -42.0
YZP O15         -49.0
YZP O16         -52.0
YZP O17         -55.0
YZP O18         -58.0
YZP O19         -61.0
YZP O20         -64.0
YZP O21         -67.0
XYP R1          -64.0
XYP R2          -61.0
XYP R3          -58.0
XYP R4          -55.0
XYP R5          -52.0
XYP R6          -49.0
XYP R7          -46.0
XYP R8          -43.0
XYP R9          -40.0
XYP R10         -37.0
XYP R11         -34.0
XYP R12         -31.0
XYP R13         -28.0
XYP R14         -25.0
XYP R15         -22.0
XYP R16         -19.0
XYP R17         -16.0
XYP R18         -13.0
XYP R19         -10.0
XYP R20         -7.0
XYP R21         -4.0
XYP R22         0.0
#if 0
YZP P1          205.0
#endif
#if 0
YZP P2          208.0
#endif
#if 0
YZP P3          211.0
#endif
#if 0
YZP P4          214.0
#endif
#if 0
YZP P5          217.0
#endif
#if 0
YZP P6          220.0
#endif
#if 0
YZP P7          223.0
#endif
#if 0
YZP P8          226.0
#endif
#if 0
YZP P9          229.0
#endif
#if 0
YZP P10         232.0
#endif
#if 0
YZP P11         235.0
```

```
#endif
#if 0
YZP P12         238.0
#endif
#if 0
YZP P13         241.0
#endif
#if 0
YZP P14         244.0
#endif
#if 0
YZP P15         247.0
#endif
#if 0
YZP P16         250.0
#endif
#if 0
YZP P17         253.0
#endif
#if 0
YZP P18         256.0
#endif
#if 0
YZP P19         259.0
#endif
#if 0
YZP P20         262.0
#endif
#if 0
YZP P21         265.0
#endif
#if 0
YZP P22         268.0
#endif
#if 0
YZP P23         271.0
#endif
#if 0
YZP P24         274.0
#endif
#if 0
XYP Q1          230.0
#endif
#if 0
XYP Q2          233.0
#endif
#if 0
XYP Q3          236.0
#endif
#if 0
XYP Q4          239.0
#endif
#if 0
XYP Q5          242.0
#endif
#if 0
XYP Q6          245.0
#endif
#if 0
XYP Q7          248.0
#endif
#if 0
XYP Q8          251.0
#endif
#if 0
XYP Q9          254.0
#endif
#if 0
XYP Q10         257.0
#endif
#if 0
```

```
XYP Q11          260.0
#endif
#if 0
XYP Q12          263.0
#endif
#if 0
XYP Q13          266.0
#endif
#if 0
XYP Q14          269.0
#endif
#if 0
XYP Q15          272.0
#endif
#if 0
XYP Q16          275.0
#endif
#if 0
XYP Q17          278.0
#endif
#if 0
XYP Q18          281.0
#endif
#if 0
XYP Q19          284.0
#endif
#if 0
XYP Q20          287.0
#endif
#if 0
XYP Q21          290.0
#endif
#if 0
XYP Q22          293.0
#endif
#if 0
XYP Q23          296.0
#endif
#if 0
XYP Q24          300.0
#endif
#if 0
YZP S1           288.0
#endif
#if 0
YZP S2           291.0
#endif
#if 0
YZP S3           294.0
#endif
#if 0
YZP S4           297.0
#endif
#if 0
YZP S5           300.0
#endif
#if 0
YZP S6           303.0
#endif
#if 0
YZP S7           306.0
#endif
#if 0
YZP S8           309.0
#endif
#if 0
YZP S9           312.0
#endif
#if 0
YZP S10          315.0
#endif
```

```
#if 0
YZP S11         318.0
#endif
#if 0
YZP S12         321.0
#endif
#if 0
YZP S13         324.0
#endif
* ------------------------------------------------------------------------------
* DOOR
* ------------------------------------------------------------------------------
RPP door1       -72.0 -46.0 2.5 182.5 -293.0 -113.0
RPP door2       -46.0 -27.5 11.0 176. -285.5 -120.5
RPP door3       -27.5 0.0 17.0 158.0 -272.5 -132.5
RPP door4       -27.5 -13.5 17.0 158.0 -272.5 -132.5
RPP doorc1      -17.0 -13.5 17.0 143.0 -257.5 -147.5
RPP doorc2      -20.5 -17.0 17.0 139.5 -254.0 -151.0
RPP doorc3      -24.0 -20.5 17.0 136.0 -250.5 -154.5
RPP doorc4      -27.5 -24.0 17.0 132.5 -247.0 -158.0
PLA dooro1      0.26 0.0 0.97 -72.0 0.0 -174.0
PLA dooro2      0.26 0.0 0.97 -72.0 0.0 -176.3
PLA dooro3      0.26 0.0 0.97 -72.0 0.0 -187.3
PLA dooro4      0.26 0.0 0.97 -72.0 0.0 -185.0
RPP doorw1      -46.0 0.0 0.0 330.0 -312.5 0.0
RPP doorw2      -18.5 0.0 85.0 140.0 -132.5 -67.0
PLA doorw3      1.75 0.0 1. -40.0 0.0 0.0
PLA doorw4      1.2 0.0 1. -46.0 0.0 -73.
XZP doorw5      95.
XZP doorw6      125.
* .............................................
*
RPP airRoom     -27.5 470.0 0.0 330.0 -302.0 -67.0
RPP air_door    -25.0 470.0 0.0 330.0 -122.0 -67.0
RPP air_cham    -180.0 0.0 0.0 330.0 -106.0 130.0
$start_translat 440.0 110.0 -184.5
SPH posito      0.0 0.0 20.0 27.5
SPH positi      0.0 0.0 20.0 27.0
RCC titani      0.0 0.0 -6. 0.0 0.0 12. 3.5
RCC grafi       0.0 0.0 -5.5 0.0 0.0 11.0 3.0
RCC core        0.0 0.0 -5.0 0.0 0.0 10.0 2.5
$end_translat
*
* ------------------------------------------------
* >>Start Beamline<<
* ------------------------------------------------
$start_transform rot35
RPP detector    -1.5 1.5 -1.5 1.5 -1.5 1.5
RPP foil1       -0.5 0.5 -0.5 0.5 -0.01 0.01
* SLIT ASSEMBLY
* ++++++++++++++++++++++++++++++
*
RPP slitass     -15. 15. -5.5 5.5 -26.9 -25.9
* move slit1
$start_translat -0.2 0.0 0.0
RPP slit1       -11. -1. -5. 5. -26.4750 -26.325
$end_translat
* move slit2
$start_translat -1.2 0.0 0.0
RPP slit2       1. 11. -5. 5. -26.475 -26.325
$end_translat
*
* Chamber
* ++++++++++++++++++++++++++++++
RCC co1         -6.5 0.0 0.0 13.0 0.0 0.0 2.5
RCC coo1        -6.5 0.0 0.0 13.0 0.0 0.0 3.75
RCC ci1         -7.4 0.0 0.0 14.8 0.0 0.0 2.35
RCC r1          -7.9 0.0 0.0 15.8 0.0 0.0 3.75
RCC co2         0.0 0.0 24.4 0.0 0.0 -40.2 2.5
RCC ci2         0.0 0.0 23.9 0.0 0.0 -41.0 2.35
RCC c21         0.0 0.0 24.4 0.0 0.0 -1.4 3.75
```

```
RCC c22          0.0 0.0 13.4 0.0 0.0 -1.4 3.75
RPP c23          -3.75 3.75 -3.75 8.25 8.7 11.2
RCC c24          0.0 0.0 7.9 0.0 0.0 -1.4 3.75
RCC c25          0.0 0.0 -6.5 0.0 0.0 -1.4 3.75
RPP c26          -3.75 3.75 -3.75 8.25 -11.2 -8.7
RCC c27          0.0 0.0 -12.0 0.0 0.0 -1.4 3.75
RCC ao1          -17.7 0.0 -26.4 35.4 0.0 0.0 11.0
RCC ai1          -16.9 0.0 -26.4 33.8 0.0 0.0 10.2
RCC ao2          0.0 0.0 -49.2 0.0 0.0 13.1 5.0
RCC ai2          0.0 0.0 -49.2 0.0 0.0 14.3 4.85
RCC ring         0.0 0.0 -45.5 0.0 0.0 3.6 7.5
* +++++++++++++++++++++++++++++++++
*
* Separation vacuum tube
* +++++++++++++++++++++++++++++++++
RPP st1          -32.0 17.0 -6.0 6.0 -49.2 -46.2
RPP stout2       -30.0 15.0 -5.0 5.0 -219.2 -49.2
RPP stin2        -30.0 15.0 -3.8 3.8 -219.2 -49.2
RPP stconj1      -30.0 15.0 -6.0 6.0 -219.2 -49.2
PLA stout3       14.6 0.0 -1.2 15.0 0.0 -49.2
PLA stout4       14.6 0.0 1.2 -30.0 0.0 -49.2
PLA stin3        14.6 0.0 -1.2 13.8 0.0 -49.2
PLA stin4        14.6 0.0 1.2 -28.8 0.0 -49.2
* +++++++++++++++++++++++++++++++++
*
* Magnet
* +++++++++++++++++++++++++++++++++
RCC magout1      142.5 -13.1 -219.2 0.0 26.2 0.0 176.75
RCC magout2      142.5 -13.1 -219.2 0.0 26.2 0.0 122.75
RCC magin1       142.5 -7.1 -219.2 0.0 14.2 0.0 171.25
RCC magin2       142.5 -7.1 -219.2 0.0 14.2 0.0 128.75
RCC mag1         142.5 -7.1 -219.2 0.0 14.2 0.0 160.0
RCC mag2         142.5 -7.1 -219.2 0.0 14.2 0.0 140.0
RCC mag3         142.5 -2.75 -219.2 0.0 5.5 0.0 160.0
RCC mag4         142.5 -2.75 -219.2 0.0 5.5 0.0 140.0
* mag-35degree
PLA pla1         0.81915 0.0 -0.57357 142.5 0.0 -219.2
* mag-55degree
PLA pla2         -0.57357 0.0 0.81915 -7.5 0.0 -219.2
* mag-55degree
PLA pla3         -0.57357 0.0 0.81915 -7.5 0.0 -191.2
* mag-55degree
PLA pla4         -0.57357 0.0 0.81915 -7.5 0.0 -187.2
YZP yzp          142.5
* +++++++++++++++++++++++++++++++++
*
* Shielding
* +++++++++++++++++++++++++++++++++
RPP shie1        -35.5 20.5 -110.0 30.0 -180.0 38.0
RPP shie2        -45.5 30.5 -110.0 38.0 -180.0 48.0
XYP shie3        -49.2
*      +++++++++++++++++++++++++++++++++
$end_transform
*
*       Separation vacuum tube (curve)
*      +++++++++++++++++++++++++++++++++
$start_translat 0.0 110.0 0.0
RCC strout1      134.0 -2.675 -23.7 0.0 5.35 0.0 164.65
RCC strout2      134.0 -2.675 -46.2 0.0 5.35 0.0 134.45
RCC strin1       134.0 -2.375 -23.7 0.0 4.75 0.0 164.05
RCC strin2       134.0 -2.375 -46.2 0.0 4.75 0.0 135.05
RPP strout3      134.0 181.0 -2.675 2.675 -188.35 -180.65
RPP strin3       134.0 180.0 -2.375 2.375 -187.75 -181.25
PLA strout4      1.2 0.0 1.0 7.8576551481 0.0 -129.5193334663
PLA strout5      1.7 0.0 1.0 15.241317067 0.0 -109.23314785
PLA strin5       1.7 0.0 1.0 15.241317067 0.0 -110.43314785
PLA strin4       1.2 0.0 1.0 7.8576551481 0.0 -128.6193334663
XZP strout6      -2.675
XZP strout7      2.675
XZP strin6       -2.375
XZP strin7       2.375
```

```
* +++++++++++++++++++++++++++++++++++
*
* Coil
* +++++++++++++++++++++++++++++++++++
RCC coil1       134.0 -7.1 -34.5 0.0 14.2 0.0 170.65
RCC coil2       134.0 -7.1 -34.5 0.0 14.2 0.0 129.35
RCC coil3       134.0 -7.1 -34.5 0.0 14.2 0.0 160.6
RCC coil4       134.0 -7.1 -34.5 0.0 14.2 0.0 139.4
XZP coil5       -1.1
XZP coil6       1.1
$end_translat
*      +++++++++++++++++++++++++++++++++++
*
* >>End Beamline<<
* ---------------------------------------------------
YZP shieyzp     -46.0
XYP shiexyp     0.0
*
* ---------------------------------------------------
* Other objects
* ---------------------------------------------------
*
RPP locker1     -307.0 -202.0 0.0 180.0 -369.0 -189.0
RPP inside1     -306.8 -202.2 0.2 179.8 -368.8 -309.2
RPP inside2     -306.8 -202.2 0.2 179.8 -308.8 -249.2
RPP inside3     -306.8 -202.2 0.2 179.8 -248.8 -189.2
RPP locker2     -307.0 -217.0 0.0 180.0 -189.0 -9.0
RPP inside4     -306.8 -217.2 0.2 179.8 -188.8 -129.2
RPP inside5     -306.8 -217.2 0.2 179.8 -128.8 -69.2
RPP inside6     -306.8 -217.2 0.2 179.8 -68.8 -9.2
* LAB bench
* ---------------------------------------------------
$start_translat -292 0.0 727.5
RPP labbase     0.0 210. 0.0 90. 0.0 150.
RPP labbase1    60. 150. 0.0 85. 0.0 150.
RPP vertsh      0.0 210. 90. 165. 72.5 77.5
RPP horish      0.0 210. 125. 130. 50. 100.
$end_translat
$start_translat -360 0.0 1039
RPP glovbase    0.0 306. 0.0 90. 15. 80.
RPP glovetop    0.0 306. 90. 213. 0.0 95.
RPP glovebox    12. 141. 100. 180. 10. 90.
RPP glovebo1    165. 294. 100. 180. 10. 90.
PLA gloside     0.0 -1. 1. 0.0 90. 0.0
PLA gloside1    0.0 1. 1. 0.0 190. 0.0
PLA gloside2    1. 0.0 1. 151. 0.0 0.0
PLA gloside3    -1. 0.0 1. 2. 0.0 0.0
XYP gloside4    10.
PLA gloside5    1. 0.0 1. 304. 0.0 0.0
PLA gloside6    -1. 0.0 1. 155. 0.0 0.0
RPP gloglass    12. 141. 100. 180. 10. 12.
RPP gloglas1    165. 294. 100. 180. 10. 12.
$end_translat
$start_translat 50.0 0.0 -67.0
RPP leadwall    0.0 8.0 80.0 145.0 -50.0 0.0
$end_translat
RPP doorw7      -46.0 0.0 0.0 330.0 -312.5 0.0
RPP door5       -27.5 0.0 17.0 158.0 -272.5 -132.5
YZP O22         -42.0
XYP R23         -22.0
XYP R24         -25.0
* ---------------------------------------------------
END
Blkbody      5 +blkbody -wall
Wall         5 +wall -air
* ---------------------------------
* Sections of the heavy concrete walls
* ---------------------------------
R1           5 +hwall4 +R1
R2           5 +hwall4 -R1 +R2
R3           5 +hwall4 -R2 +R3
```

```
R4              5 +hwall4 -R3 +R4
R5              5 +hwall4 -R4 +R5
R6              5 +hwall4 -R5 +R6
R7              5 +hwall4 -R6 +R7
R8              5 +hwall4 -R7 +R8
R9              5 +hwall4 -R8 +R9
R10             5 +hwall4 -R9 +R10
R11             5 +hwall4 -R10 +R11
R12             5 +hwall4 -R11 +R12
R13             5 +hwall4 -R12 +R13
R14             5 +hwall4 -R13 +R14
R15             5 +hwall4 -R14 +R15
R16             5 +hwall4 -R15 +R16
R17             5 +hwall4 -R16 +R17
R18             5 +hwall4 -R17 +R18
R19             5 +hwall4 -R18 +R19
R20             5 +hwall4 -R19 +R20
R21             5 +hwall4 -R20 +R21
R22             5 +hwall4 -R21 +R22
#if 0
P1              5 +hwall2 +P1
#endif
#if 0
P2              5 +hwall2 -P1 +P2
#endif
#if 0
P3              5 +hwall2 -P2 +P3
#endif
#if 0
P4              5 +hwall2 -P3  +P4
#endif
#if 0
P5              5 +hwall2 -P4 +P5
#endif
#if 0
P6              5 +hwall2 -P5+P6
#endif
#if 0
P7              5 +hwall2 -P6+P7
#endif
#if 0
P8              5 +hwall2 -P7+P8
#endif
#if 0
P9              5 +hwall2 -P8 +P9
#endif
#if 0
P10             5 +hwall2 -P9 +P10
#endif
#if 0
P11             5 +hwall2-P10 +P11
#endif
#if 0
P12             5 +hwall2-P11 +P12
#endif
#if 0
P13             5 +hwall2-P12 +P13
#endif
#if 0
P14             5 +hwall2-P13 +P14
#endif
#if 0
P15             5 +hwall2-P14 +P15
#endif
#if 0
P16             5 +hwall2-P15 +P16
#endif
#if 0
P17             5 +hwall2-P16 +P17
#endif
#if 0
```

```
P18             5 +hwall2 -P17 +P18
#endif
#if 0
P19             5 +hwall2 -P18 +P19
#endif
#if 0
P20             5 +hwall2 -P19 +P20
#endif
#if 0
P21             5 +hwall2 -P20 +P21
#endif
#if 0
P22             5 +hwall2 -P21 +P22
#endif
#if 0
P23             5 +hwall2 -P22 +P23
#endif
#if 0
P24             5 +hwall2 -P23 +P24
#endif
#if 0
P25             5 +hwall2 -P24
#endif
#if 0
Q1              5 +hwall3+Q1
#endif
#if 0
Q2              5 +hwall3 -Q1 +Q2
#endif
#if 0
Q3              5 +hwall3 -Q2 +Q3
#endif
#if 0
Q4              5 +hwall3 -Q3 +Q4
#endif
#if 0
Q5              5 +hwall3 -Q4 +Q5
#endif
#if 0
Q6              5 +hwall3 -Q5 +Q6
#endif
#if 0
Q7              5 +hwall3 -Q6 +Q7
#endif
#if 0
Q8              5 +hwall3 -Q7 +Q8
#endif
#if 0
Q9              5 +hwall3 -Q8 +Q9
#endif
#if 0
Q10             5 +hwall3 -Q9 +Q10
#endif
#if 0
Q11             5 +hwall3 -Q10 +Q11
#endif
#if 0
Q12             5 +hwall3 -Q11 +Q12
#endif
#if 0
Q13             5 +hwall3 -Q12 +Q13
#endif
#if 0
Q14             5 +hwall3 -Q13 +Q14
#endif
#if 0
Q15             5 +hwall3 -Q14 +Q15
#endif
#if 0
Q16             5 +hwall3 -Q15 +Q16
#endif
```

```
#if 0
Q17             5 +hwall3-Q16 +Q17
#endif
#if 0
Q18             5 +hwall3-Q17 +Q18
#endif
#if 0
Q19             5 +hwall3-Q18 +Q19
#endif
#if 0
Q20             5 +hwall3-Q19 +Q20
#endif
#if 0
Q21             5 +hwall3-Q20 +Q21
#endif
#if 0
Q22             5 +hwall3-Q21 +Q22
#endif
#if 0
Q23             5 +hwall3-Q22 +Q23
#endif
#if 0
Q24             5 +hwall3-Q23 +Q24
#endif
#if 0
Q25             5 +hwall3-Q24
#endif
#if 0
s1              5 +hwall1+S2
#endif
#if 0
s2              5 +hwall1-S2 +S3
#endif
#if 0
s3              5 +hwall1-S3 +S4
#endif
#if 0
s4              5 +hwall1-S4 +S5
#endif
#if 0
s5              5 +hwall1-S5 +S6
#endif
#if 0
s6              5 +hwall1-S6 +S7
#endif
#if 0
s7              5 +hwall1-S7 +S8
#endif
#if 0
s8              5 +hwall1-S8 +S9
#endif
#if 0
s9              5 +hwall1-S9 +S10
#endif
#if 0
s10             5 +hwall1-S10 +S11
#endif
#if 0
s11             5 +hwall1-S11 +S12
#endif
#if 0
s12             5 +hwall1-S12 +S13
#endif
#if 0
s13             5 +hwall1-S13
#endif
Heavwall        5 |+hwall1 |+hwall2 |+hwall3 |+hwall5 -hwall6
Air             5 +air -hwall1 -hwall2 -hwall3 -hwall4 -hwall5 -airRoom -air_cham
                                -locker1 -locker2 -labbase -horish
                  -vertsh -glovbase -glovetop -door1 -doorw1
                  | +inside1
```

```
                | +inside2
                | +inside3
                | +inside4
                | +inside5
                | +inside6
                | +labbase1
                | +glovebox -gloglass
                | +glovebo1 -gloglas1
                | +glovetop +gloside4+gloside +gloside1+gloside2 +gloside3
                | +glovetop +gloside4 +gloside +gloside1 +gloside5 +gloside6
                | +hwall6 -doorw1
Airchem      5 +stout4 +shie1 -st1 -airRoom -doorw1
                |+stout4 +shie1 -st1 -airRoom -doorw2 -doorw4 +doorw1 +doorw6 -doorw5
                | +shie1 -hwall4 -st1 -stout3 -airRoom -ao1 -doorw1
                | +shie1 -hwall4 -st1 -stout3 -airRoom -ao1 +doorw1 +doorw3 +doorw6 -doorw5
                | +stout3 +shie1 +shie3 -stout2 -stout4 -airRoom -doorw1
                | +stout3 +shie1 +shie3 -stout2 -stout4 -airRoom +doorw1 +doorw6 -doorw5
                | +stout3 +shie1 -c23 -c26 -st1 -stout4 -shie3 -ring -ao1 -ao2
                          -co2 -c27 -c25 -r1 -c24 -c22 -c21
                | +coo1 -co1 -co2
                | +air_cham -shie2 -shiexyp
                | +air_cham +shieyzp +shiexyp -shie2 -doorw1
ACTRoom      5 +airRoom -magout1 -leadwall -posito -doorw1
                | +airRoom -pla1 -strout3 -leadwall -posito
                | +airRoom +magout2 -leadwall
                | +airRoom +magout1 +pla3 -magout2 -pla2 -strout5
                | +magout1 +pla3 +strout4 +airRoom -pla2
                | +magout1 +pla4 +airRoom -stconj1 -pla3
                | +stout4 +magout1 +airRoom -pla4 -doorw4
                | +magout1 +airRoom -stout4 -stout2 -doorw2 +doorw1
                | +stout4 +magout1 +airRoom -pla4 +doorw4 +doorw2
                | +airRoom -stout3 -pla4 +doorw2
                | +airRoom -stout3 -pla4 +magout1
                | +pla3 +strout5 +airRoom -pla2 -strout4 -strout7 +doorw2
                | +pla3 +strout5 +strout6 +airRoom -pla2 -strout4 +doorw2
                | +pla3 +strout5 +airRoom -pla2 -strout4 -strout7 -doorw2 +magout1
                | +pla3 +strout5 +strout6 +airRoom -pla2 -strout4 -doorw2 +magout1
                | +stout3 +magout1 +airRoom -stout2 -pla4 +doorw2
                | +door3 -door4
                | +doorw2 -magout1
                | +door4
                | +airRoom +doorw1 -doorw2 -magout1 -doorw4 +doorw6 -doorw5
Shield       5 +shie2 -shie1 +shieyzp
                | +shie2 -shie1 -shiexyp
Door1        5 +door1 -O15
Door2        5 +door1 +O15 -O16
Door3        5 +door1 +O16 -O17
Door4        5 +door1 +O17 -O18
Door5        5 +door1 +O18 -O19
Door6        5 +door1 +O19 -O20
Door7        5 +door1 +O20 -O21
Door8        5 +door1 +O21
DoorW1       5 +doorw1 -door3 -doorw2 -O1 +R1 -doorw6
                |+doorw1 -door3 -doorw2 -O1 +R1 +doorw5
                |+doorw1 -door3 -doorw2 -O1 +R1 +doorw6 -doorw5 -doorw3
                |+doorw1 -door3 -doorw2 -O1 +doorw6 -doorw5 +doorw4
DoorW2       5 +doorw1 -door3 -doorw2 +O1 -O2 +R2 -doorw6
                | +doorw1 -R1 +R2 -O1 -doorw6
                | +doorw1 -door3 -doorw2 +O1 -O2 +R2 +doorw5
                | +doorw1 -R1 +R2 -O1 +doorw5
                | +doorw1 -door3 -doorw2 +O1 -O2 +R2 +doorw6 -doorw5 -doorw3
                | +doorw1 -R1 +R2 -O1 +doorw6 -doorw5
                | +doorw1 -door3 -doorw2 +O1 -O2 +doorw6 -doorw5 +doorw4
DoorW3       5 +doorw1 -door3 -doorw2 +O2 -O3 +R3 -doorw6
                | +doorw1 -R2 +R3 -O2 -doorw6
                | +doorw1 -door3 -doorw2 +O2 -O3 +R3 +doorw5
                | +doorw1 -R2 +R3 -O2 +doorw5
                | +doorw1 -door3 -doorw2 +O2 -O3 +R3 +doorw6 -doorw5 -doorw3
                | +doorw1 -R2 +R3 -O2 +doorw6 -doorw5 -doorw3
                | +doorw1 -door3 -doorw2 +O2 -O3 +doorw6 -doorw5 +doorw4
DoorW4       5 +doorw1 -door3 -doorw2 +O3 -O4 +R4 -doorw6
```

```
                | +doorw1 −R3 +R4 −O3 −doorw6
                | +doorw1 −door3 −doorw2 +O3 −O4 +R4 +doorw5
                | +doorw1 −R3 +R4 −O3 +doorw5
                | +doorw1 −R3 +R4 +doorw6 −doorw5 −doorw3
                | +doorw1 −door3 −doorw2 +O3 −O4+doorw6 −doorw5 +doorw4
DoorW5      5 +doorw1 −door3 −doorw2 +O4 −O5 +R5 −doorw6
                | +doorw1 −R4 +R5 −O4 −doorw6
                | +doorw1 −door3 −doorw2 +O4 −O5 +R5 +doorw5
                | +doorw1 −R4 +R5 −O4 +doorw5
                | +doorw1 −R4 +R5 +doorw6 −doorw5 −doorw3
                | +doorw1 −door3 −doorw2 +O4 −O5 +doorw6 −doorw5 +doorw4
DoorW6      5 +doorw1 −door3 −doorw2 +O5 −O6 +R6 −doorw6
                | +doorw1 −R5 +R6 −O5 −doorw6
                | +doorw1 −door3 −doorw2 +O5 −O6 +R6 +doorw5
                | +doorw1 −R5 +R6 −O5 +doorw5
                | +doorw1 −R5 +R6 +doorw6 −doorw5 −doorw3
                | +doorw1 −door3 −doorw2 +O5 −O6 +doorw6 −doorw5 +doorw4
DoorW7      5 +doorw1 −door3 −doorw2 +O6 −O7 +R7 −doorw6
                | +doorw1 −R6 +R7 −O6 −doorw6
                | +doorw1 −door3 −doorw2 +O6 −O7 +R7 +doorw5
                | +doorw1 −R6 +R7 −O6 +doorw5
                | +doorw1 −R6 +R7 +doorw6 −doorw5 −doorw3
                | +doorw1 −door3 −doorw2 +O6 −O7 +doorw6 −doorw5 +doorw4
DoorW8      5 +doorw1 −door3 +O7 −O8 +R8 −doorw6
                | +doorw1 −R7 +R8 −O7 −doorw6
                | +doorw1 −door3 +O7 −O8 +R8 +doorw5
                | +doorw1 −R7 +R8 −O7 +doorw5
                | +doorw1 −R7 +R8 +doorw6 −doorw5 −doorw3
                | +doorw1 −door3 +O7 −O8 +doorw6 −doorw5 +doorw4
DoorW9      5 +doorw1 −door3 +O8 −O9 +R9 −doorw6
                | +doorw1 −R8 +R9 −O8 −doorw6
                | +doorw1 −door3 +O8 −O9 +R9 +doorw5
                | +doorw1 −R8 +R9 −O8 +doorw5
                | +doorw1 −R8 +R9 +doorw6 −doorw5 −doorw3
                | +doorw1 −door3 +O8 −O9 +doorw6 −doorw5 +doorw4
DoorW10     5 +doorw1 −door3 +O9 −O10 +R10 −doorw6
                | +doorw1 −R9 +R10 −O9 −doorw6
                | +doorw1 −door3 +O9 −O10 +R10 +doorw5
                | +doorw1 −R9 +R10 −O9 +doorw5
                | +doorw1 −R9 +R10 +doorw6 −doorw5 −doorw3
                | +doorw1 −door3 +O9 −O10 +doorw6 −doorw5 +doorw4
DoorW11     5 +doorw1 −door3 +O10 −O11 +R11 −doorw6
                | +doorw1 −R10 +R11 −O10 −doorw6
                | +doorw1 −door3 +O10 −O11 +R11 +doorw5
                | +doorw1 −R10 +R11 −O10 +doorw5
                | +doorw1 −R10 +R11 +doorw6 −doorw5 −doorw3
                | +doorw1 −door3 +O10 −O11 +doorw6 −doorw5 +doorw4
DoorW12     5 +doorw1 −door3 +O11 −O12 +R12 −doorw6
                | +doorw1 −R11 +R12 −O11 −doorw6
                | +doorw1 −door3 +O11 −O12 +R12 +doorw5
                | +doorw1 −R11 +R12 −O11 +doorw5
                | +doorw1 −R11 +R12 +doorw6 −doorw5 −doorw3
                | +doorw1 −door3 +O11 −O12 +doorw6 −doorw5 +doorw4
DoorW13     5 +doorw1 −door3 +O12 −O13 +R13 −doorw6
                | +doorw1 −R12 +R13 −O12 −doorw6
                | +doorw1 −door3 +O12 −O13 +R13 +doorw5
                | +doorw1 −R12 +R13 −O12 +doorw5
                | +doorw1 −R12 +R13 +doorw6 −doorw5 −doorw3
                | +doorw1 −door3 +O12 −O13 +doorw6 −doorw5 +doorw4
DoorW14     5 +doorw1 −door3 +O13 −O14 +R14 −doorw6
                | +doorw1 −R13 +R14 −O13 −doorw6
                | +doorw1 −door3 +O13 −O14 +R14 +doorw5
                | +doorw1 −R13 +R14 −O13 +doorw5
                | +doorw1 −R13 +R14 +doorw6 −doorw5 −doorw3
                | +doorw1 −door3 +O13 −O14 +doorw6 −doorw5 +doorw4
DoorW15     5 +doorw1 −door3 +O14 +R15 −doorw6
                | +doorw1 −R14 +R15 −O14 −doorw6
                | +doorw1 −door3 +O14 +R15 +doorw5
                | +doorw1 −R14 +R15 −O14 +doorw5
                | +doorw1 −R14 +R15 +doorw6 −doorw5 −doorw3
                | +doorw1 −door3 +O14 −O15 +doorw6 −doorw5 +doorw4
```

```
DoorW16         5 +doorw1 -door3 -R15 +R16 -doorw6
                  |+doorw1 -door3 -R15 +R16 +doorw5
                  |+doorw1 -R15 +R16 +doorw6 -doorw5 -doorw3
DoorW17         5 +doorw1 -door3 -R16 +R17 -doorw6
                  |+doorw1 -door3 -R16 +R17 +doorw5
                  |+doorw1 -R16 +R17 +doorw6 -doorw5 -doorw3
DoorW18         5 +doorw1 -door3 -R17 +R18 -doorw6
                  |+doorw1 -door3 -R17 +R18 +doorw5
                  |+doorw1 -R17 +R18 +doorw6 -doorw5 -doorw3
DoorW19         5 +doorw1 -door3 -R18 +R19 -doorw6
                  |+doorw1 -door3 -R18 +R19 +doorw5
                  |+doorw1 -R18 +R19 +doorw6 -doorw5 -doorw3
DoorW20         5 +doorw1 -door3 -R19 +R20 -doorw6
                  |+doorw1 -door3 -R19 +R20 +doorw5
                  |+doorw1 -R19 +R20 +doorw6 -doorw5 -doorw3
DoorW21         5 +doorw1 -door3 -R20 +R21 -doorw6
                  |+doorw1 -door3 -R20 +R21 +doorw5
                  |+doorw1 -R20 +R21 +doorw6 -doorw5 -doorw3
DoorW22         5 +doorw1 -door3 -R21 -doorw6
                  |+doorw1 -door3 -R21 +doorw5
                  |+doorw1 -R21 +doorw6 -doorw5 -doorw3
* ------------------------------------------------------------
* BEAM FRONT END
* ------------------------------------------------------------
Titani          5 +titani -grafi
Grafi           5 +grafi -core
Core            5 +core
Posito          5 +posito -positi
Positi          5 +positi-titani
*
* ------------------------------------------------------------
* >>Start Beamline<<
* ------------------------------------------------------------
*
chamber         5 +(+r1 -ci1 -(+coo1 -co1) -ci2) | +(+co2 |  +c21 |  +c22 |  +c23 |
                                  +c24 |  +c25 |  +c26 |  +c27)
                  -ci2 -ci1
                  | +ao1 -ai1 -co2 -ci2 -ai2
                  | +(+ao2 |  +ring) -ai2 -ao1 -st1
Mag             5 +(+(+magout1 -magin1 -magout2) | +(+magin2 -magout2) |
                                  +(+mag1 -mag2 -mag3))
                                  +pla1 +pla2 +yzp
St              5 +stout2 +stout3 -stin2 -stout4 -pla4
                  | +stout2 +stout3 -stin3 -pla4
                  | +stout2 +stin4 -stout4 -pla4
                  | +st1 -ai2
Str             5 +strout1 -strin1 -strout2 +pla2 +yzp +pla1
                  | +strin2 -strout2 +pla2 +yzp +pla1
                  | +pla3 +strin5 +strin4 +strin7 -pla2 -strout4 -strin6
                  | +pla3 +strin5 +strin4 +strout7 -pla2 -strout4 -strin7
                  | +pla3 +strin5 +strin4 +strin6 -pla2 -strout4 -strout6
                  | +pla3 +strin5 +strout7 -pla2 -strin4 -strin7
                  | +pla3 +strin5 +strin6 -pla2 -strin4 -strout6
                  | +pla3 +strout5 +strin7 -pla2 -strin5 -strin4 -strin6
                  | +pla3 +strout5 +strout7 -pla2 -strin5 -strin4 -strin7
                  | +pla3 +strout5 +strin6 -pla2 -strin5 -strin4 -strout6
                  | +stconj1 +pla4 +strin7 -stin3 -pla3 -strin6
                  | +stconj1 +pla4 -stin3 -pla3 -strin7
                  | +stconj1 +pla4 +strin6 -stin3 -pla3
                  | +stconj1 +stin3 +pla4 -pla3 -strin7
                  | +stconj1 +stin3 +pla4 +strin6 -pla3
                  | +stconj1 +stin4 +pla4 +strin7 -pla3 -strin6
                  | +strout3 -pla1 -strin3
Magfield        5 +pla1 +pla2 +yzp +strin1 -strin2
Vacuum          5 +pla3 +strin5 +strin7 -pla2 -strin4 -strin6
                  | +ai1-slitass
                  | +ai2
                  | +ci1 -detector
                  | +ci2 -detector
                  | +strin3 -pla1
                  | +stin2 +stin3 -stin4 -pla4
```

```
                | +stin3 +pla4 +strin7 -stin4 -pla3 -strin6
Coil          5 +pla1 +pla2 +coil1 -coil2 -coil3 -coil4 -coil6 +yzp
                | +pla1 +pla2 +coil1 +coil5 -coil2 -coil3 -coil4 +yzp
                | +pla1 +pla2 +coil1 +coil3 +coil4 -coil2 -coil6 +yzp
                | +pla1 +pla2 +coil1 +coil3 +coil4 +coil5 -coil2 +yzp
Air_coil      5 +magin1 +pla1 +pla2 +yzp -coil1
                | +pla1 +pla2 +yzp +coil3 -mag1
                | +pla1 +pla2 +yzp +coil1 +coil6 -coil3 -coil5
                | +mag3 +pla1 +pla2 +yzp -mag2 -strout1
                | +pla1 +pla2 +yzp +strout2 -mag2
                | +mag2 +pla1 +pla2 +yzp -coil4
                | +pla1 +pla2 +yzp +coil4 +coil6 -coil2 -coil5
                | +pla1 +pla2 +yzp +coil2 -magin2
*
* ----------------------------------------------------------
* Other objects
* ----------------------------------------------------------
*
Locker        5 +locker1 -inside1 -inside2 -inside3
                | +locker2 -inside4 -inside5 -inside6
Foil          5 +foil1
Detector      5 +detector -foil1
Slit          5 +slit1
                |+slit2
Slitass       5 +slitass -slit1 -slit2
Labbench      5 +labbase -labbase1
                |+vertsh
                |+horish
Glovebox      5 +glovbase
                |+glovetop -glovebox -glovebo1 -(+gloside4+gloside +gloside1+gloside2 +gloside3)-
                          ( +gloside4 +gloside +gloside1 +gloside5 +gloside6 )
GlovGlas      5 +gloglas1 |+gloglass
LeadWall      5 +leadwall-hwall4
* >>End Beamline<<
* ----------------------------------------------------------
*
END
GEOEND
* ----------------------------------------------------------
*
* >>Define Material<<
* ----------------------------------------------------------
MATERIAL                                 8.00                                  STEEL
COMPOUND     0.977169       IRON    0.022831     CARBON                        STEEL
MATERIAL                                 2.30                                  CONCRETE
COMPOUND     0.168038   HYDROGEN    0.563183     OXYGEN   0.021365     SODIUMCONCRETE
COMPOUND     0.021365   ALUMINUM    0.203231    SILICON   0.018595   CALCIUMCONCRETE
COMPOUND     0.004246       IRON                                              CONCRETE
MATERIAL                                 3.9                                   HEAVYCON
COMPOUND        0.002   HYDROGEN       0.31     OXYGEN      0.001     SODIUMHEAVYCON
COMPOUND        0.003   ALUMINUM      0.029    SILICON      0.004   CALCIUMHEAVYCON
COMPOUND         0.65       IRON      0.001  MAGNESIU                       HEAVYCON
MATERIAL            6.     12.011       2.26                                  Graphite
* Tantaluns
MATERIAL           73.   180.9479     16.654        18.                        TANTALUM
MATERIAL           73.   180.9479        6.0                                   tantalum
MATERIAL           92.                 18.95                                  URANIUM
MATERIAL                                 7.0                                   UC2
COMPOUND           1.0    URANIUM        2.0   Graphite                        UC2
LOW-MAT      Graphite          6.        -3.       296.                        CARBON
LOW-MAT      TANTALUM         73.       181.       296.                        TANTALUM
LOW-MAT      tantalum         73.       181.       296.                        TANTALUM
LOW-MAT       URANIUM         92.       235.        87.                        235-U
LOW-MAT      TITANIUM         22.        -2.       296.                        TITANIUM
* ----------------------------------------------------------
*
* >>Assign Material<<
* ----------------------------------------------------------
ASSIGNMA     BLCKHOLE    Blkbody
ASSIGNMA     CONCRETE        Wall
ASSIGNMA     HEAVYCON    Heavwall
```

```
ASSIGNMA    HEAVYCON          R1         R22
ASSIGNMA         AIR         Air
ASSIGNMA       STEEL       Door1       Door8
ASSIGNMA       STEEL       DoorW1      DoorW22
ASSIGNMA         AIR      ACTRoom
ASSIGNMA         AIR      Airchem
ASSIGNMA       STEEL      Shield
* ---------------------------------------------------------------------
* BEAM FRONT END
* ---------------------------------------------------------------------
ASSIGNMA    BLCKHOLE      Posito                                    VACUUM
ASSIGNMA         AIR      Positi
ASSIGNMA    TITANIUM      Titani
ASSIGNMA    Graphite       Grafi
ASSIGNMA    TITANIUM        Core
*
* ---------------------------------------------------------------------
*
* Beamline
* ++++++++++++++++++++++++++++
*
ASSIGNMA      VACUUM     Vacuum
ASSIGNMA      VACUUM    Magfield                          1.
*MGNFIELD       30.0       0.001        0.01          -0.003196
ASSIGNMA       STEEL    chamber
ASSIGNMA       STEEL         St
ASSIGNMA       STEEL        Str
ASSIGNMA       STEEL        Mag
ASSIGNMA      COPPER       Coil
ASSIGNMA         AIR   Air_coil
ASSIGNMA       STEEL     Locker
ASSIGNMA       STEEL   Labbench
ASSIGNMA        LEAD   Glovebox
ASSIGNMA        LEAD   GlovGlas
ASSIGNMA       STEEL       Foil
ASSIGNMA      VACUUM   Detector
ASSIGNMA       STEEL       Slit
ASSIGNMA      VACUUM    Slitass
ASSIGNMA        LEAD   LeadWall
RADDECAY          1.         1.        3.0                                1.
LOW-NEUT
IONTRANS    HEAVYION
*MULSOPT          1.
* ------------------
* Right wall
* ------------------
BIASING           0.0        1.0     0.0001    Blkbody   @LASTREG        1.0
BIASING           0.0        1.0     0.0005         R1
BIASING           0.0        1.0     0.0010         R2
BIASING           0.0        1.0     0.0020         R3
BIASING           0.0        1.0     0.0040         R5
BIASING           0.0        1.0     0.0080         R6         R6
BIASING           0.0        1.0     0.0160         R7
BIASING           0.0        1.0     0.0320         R8
BIASING           0.0        1.0     0.0640         R9
BIASING           0.0        1.0     0.1280        R10
BIASING           0.0        1.0     0.2560        R11
BIASING           0.0        1.0     0.5120        R12
BIASING           0.0        1.0     1.0240        R13
BIASING           0.0        1.0     2.0480        R14
BIASING           0.0        1.0     4.0960        R15
BIASING           0.0        1.0     8.1920        R16
BIASING           0.0        1.0    16.3840        R17
BIASING           0.0        1.0    32.7680        R18
BIASING           0.0        1.0    65.5360        R19
BIASING           0.0        1.0   131.0720        R20
BIASING           0.0        1.0   262.1440        R21
BIASING           0.0        1.0   524.2880        R22
* ---------------------------------
* Steel wall and door
* ---------------------------------
```

```
BIASING          0.0          1.0       0.0005      DoorW1
BIASING          0.0          1.0       0.0010      DoorW2
BIASING          0.0          1.0       0.0020      DoorW3
BIASING          0.0          1.0       0.0040      DoorW4
BIASING          0.0          1.0       0.0080      DoorW5
BIASING          0.0          1.0       0.0160      DoorW6
BIASING          0.0          1.0       0.0320      DoorW7
BIASING          0.0          1.0       0.0640      DoorW8
BIASING          0.0          1.0       0.1280      DoorW9
BIASING          0.0          1.0       0.2560     DoorW10
BIASING          0.0          1.0       0.5120     DoorW11
BIASING          0.0          1.0       1.0240     DoorW12
BIASING          0.0          1.0       2.0480     DoorW13
BIASING          0.0          1.0       4.0960     DoorW14
BIASING          0.0          1.0       8.1920     DoorW15
BIASING          0.0          1.0      16.3840     DoorW16
BIASING          0.0          1.0      32.7680     DoorW17
BIASING          0.0          1.0      65.5360     DoorW18
BIASING          0.0          1.0     131.0720     DoorW19
BIASING          0.0          1.0     262.1440     DoorW20
BIASING          0.0          1.0     524.2880     DoorW21
BIASING          0.0          1.0     1048.576     DoorW22
BIASING          0.0          1.0     2097.152       Door1
BIASING          0.0          1.0     4194.304       Door2
BIASING          0.0          1.0     8388.608       Door3
BIASING          0.0          1.0    16777.216       Door4
BIASING          0.0          1.0    33554.432       Door5
BIASING          0.0          1.0      40000.0       Door6
BIASING          0.0          1.0      60000.0       Door7
BIASING          0.0          1.0      80000.0       Door8
* ---------------------------------------------------------------
* Experimental hall, air, and heavy wall
* ---------------------------------------------------------------
BIASING          0.0          1.0      90000.0   Heavwall    Airchem
BIASING          0.0          1.0      90000.0     Shield     Shield
* ---------------------------------------------------------
* Glovebox, lab bench, locker
* ---------------------------------------------------------
BIASING          0.0          1.0      90000.0   Glovebox   GlovGlas
BIASING          0.0          1.0      90000.0   Labbench   Labbench
BIASING          0.0          1.0      90000.0     Locker     Locker
* ------------------------------------------------------
* Beamline, detector and slits
* ------------------------------------------------------
BIASING          0.0          1.0       0.0005         St     Vacuum
BIASING          0.0          1.0       0.0005       Foil    Slitass
BIASING          0.0          1.0       0.0005    chamber
*BIASING         0.0
*BIASING         0.0
*BIASING         0.0
*BIASING         0.0
*BIASING         0.0
*BIASING         0.0
*BIASING         0.0
*BIASING         0.0
*BIASING         0.0
*BIASING         0.0
*BIASING         0.0
*
* ************************************************
*
IRRPROFI     64800.0         3E13
*DCYTIMES    -3.24E4      -2.88E4      -2.52E4      -2.16E4      -1.80E4      -1.44E4
DCYTIMES     -1.08E4      -7.20E3      -3.60E3          0.0       3.60E3       7.20E3
DCYTIMES      1.08E4       1.44E4       1.80E4       2.16E4       2.52E4       2.88E4
DCYTIMES      3.24E4       3.60E4
* ************************************************************
*USRBIN          10.   BEAMPART        -21.        150.        115.       100.0beampart
*USRBIN        -130.0        105.      -210.        400.         10.       300.0 &
*USRBIN          10.   BEAMPART        -22.        -60.        115.        70.0beampar1
*USRBIN        -120.0        105.         0.        400.         10.       300.0 &
```

```
*DCYSCORE          1.                                    Activ1    Activ1          USRBIN
*USRBIN            0.0  ACTIVITY      -40.      441.0      111.    -180.0Activ1
*USRBIN          439.0       109.    -189.0        2.0        2.0       2.0 &
*DCYSCORE          2.                                    Activ2    Activ2          USRBIN
*USRBIN            0.0  ACTIVITY      -40.      441.0      111.    -180.0Activ2
*USRBIN          439.0       109.    -189.0        2.0        2.0       9.0 &
*DCYSCORE          3.                                    Activ3    Activ3          USRBIN
*USRBIN            0.0  ACTIVITY      -40.      441.0      111.    -180.0Activ3
*USRBIN          439.0       109.    -189.0        2.0        2.0       9.0 &
*DCYSCORE          4.                                    Activ4    Activ4          USRBIN
*USRBIN            0.0  ACTIVITY      -40.      441.0      111.    -180.0Activ4
*USRBIN          439.0       109.    -189.0        2.0        2.0       9.0 &
*DCYSCORE          5.                                    Activ5    Activ5          USRBIN
*USRBIN            0.0  ACTIVITY      -40.      441.0      111.    -180.0Activ5
*USRBIN          439.0       109.    -189.0        2.0        2.0       9.0 &
*DCYSCORE          6.                                    Activ6    Activ6          USRBIN
*USRBIN            0.0  ACTIVITY      -40.      441.0      111.    -180.0Activ6
*USRBIN          439.0       109.    -189.0        2.0        2.0       9.0 &
*DCYSCORE          7.                                    Activ7                    USRBIN
*USRBIN            0.0  ACTIVITY      -40.      441.0      111.    -180.0Activ7
*USRBIN          439.0       109.    -189.0        2.0        2.0       9.0 &
*DCYSCORE          8.                                    Activ8    Activ8          USRBIN
*USRBIN            0.0  ACTIVITY      -40.      441.0      111.    -180.0Activ8
*USRBIN          439.0       109.    -189.0        2.0        2.0       9.0 &
*DCYSCORE          9.                                    Activ9    Activ9          USRBIN
*USRBIN            0.0  ACTIVITY      -40.      441.0      111.    -180.0Activ9
*USRBIN          439.0       109.    -189.0        2.0        2.0       9.0 &
*DCYSCORE         10.                                    Activ10   Activ10         USRBIN
*USRBIN            0.0  ACTIVITY      -40.      441.0      111.    -180.0Activ10
*USRBIN          439.0       109.    -189.0        2.0        2.0       9.0 &
*DCYSCORE         11.                                    Activ11   Activ11         USRBIN
*USRBIN            0.0  ACTIVITY      -40.      441.0      111.    -180.0Activ11
*USRBIN          439.0       109.    -189.0        2.0        2.0       9.0 &
*DCYSCORE         12.                                    Activ12   Activ12         USRBIN
*USRBIN            0.0  ACTIVITY      -40.      441.0      111.    -180.0Activ12
*USRBIN          439.0       109.    -189.0        2.0        2.0       9.0 &
*DCYSCORE         13.                                    Activ13   Activ13         USRBIN
*USRBIN            0.0  ACTIVITY      -40.      441.0      111.    -180.0Activ13
*USRBIN          439.0       109.    -189.0        2.0        2.0       9.0 &
*DCYSCORE         14.                                    Activ14   Activ14          1.USRBIN
*USRBIN            0.0  ACTIVITY      -40.      441.0      111.    -180.0Activ14
*USRBIN          439.0       109.    -189.0        2.0        2.0       9.0 &
* Dose-------------------------------------------------------------------
DCYSCORE           5.                                    EqDose1   EqDose5         USRBIN
AUXSCORE       USRBIN   ALL-PART                         EqDose1   EqDose5         AMB74
USRBIN            10.    DOSE-EQ       -27.      470.0      330.    1130.EqDose1
USRBIN          -400.0       0.0     -400.0      300.0      300.     300.0 &
USRBIN            10.    DOSE-EQ       -28.       80.0      130.      60.0EqDose5
USRBIN          -150.0      90.0     -140.0      250.0      250.     250.0 &
*DCYSCORE          7.                                    EqDose2   EqDose2         USRBIN
*USRBIN           10.    DOSE-EQ       -23.      200.0      330.     300.0EqDose2
*USRBIN         -300.0       0.0     -300.0      250.0      150.     300.0 &
*DCYSCORE         11.                                    EqDose3   EqDose3         USRBIN
*USRBIN           10.    DOSE-EQ       -24.      200.0      330.     300.0EqDose3
*USRBIN         -300.0       0.0     -300.0      250.0      150.     300.0 &
*DCYSCORE         11.                                    EqDose4   EqDose4         USRBIN
*USRBIN           10.    DOSE-EQ       -24.      200.0      330.     300.0EqDose4
*USRBIN         -300.0       0.0     -300.0      250.0      150.     300.0 &
*DCYSCORE         11.                          ResNUCLEI2                         RESNUCLE
*
* TEST
* ----------------
*
*RESNUCLE          3.       -25.                                  Core          ResNUCLEI1
*RESNUCLE          3.        26.                                  Core          ResNUCLEI2
*USRBIN            10.  BEAMPART       -24.      470.0      330.    -100.0P Beam
*USRBIN          300.0       0.0     -400.0       200.       200.      200. &
* ++++++++++++++++++++++++++++
*
* Set the random number seed
RANDOMIZ           1.       10.0
```

```
* Set the number of primary histories to be simulated in the run
START         125.0E6
STOP
```

DEPARTEMENT NATUURKUNDE EN STERRENKUNDE
Celestijnenlaan 200d bus 2412
3001 HEVERLEE, BELGIË
tel. + 32 16 32 71 24
fys.kuleuven.be